Apparent superluminal separation velocities of the components of extragalactic objects

L. I. Matveenko

Institute of Space Research, Academy of Sciences of the USSR
Usp. Fiz. Nauk **140**, 463–501 (July 1983)

Objects with active nuclei are reviewed. Their fine structure and its variation in time are considered. In a number of objects, velocities of the components exceeding the velocity of light are observed. Models that explain this phenomenon are discussed.

PACS numbers: 98.70. – f

CONTENTS

1. INTRODUCTION

The last decade was marked by a sensational discovery—motions of components with velocity exceeding the velocity of light were discovered in a number of radio sources. What are these objects and what is their nature?

Radio astronomers studied the spectra of radio sources and, as they mastered first short centimeter wavelengths, and then millimeter wavelengths, they noted that some of the sources do not have the ordinary power-law spectra of the type $F \sim \nu^{\alpha}$, where F is the flux density of the radio radiation, ν is the frequency, and α is the spectral index, but contain high-frequency excesses. Figure 1 shows the power-law spectrum of the giant elliptic galaxy Virgo A and spectra with high-frequency excesses—of the quasar 3C 273 and the Seyfert galaxy 3C 84.[1,2]

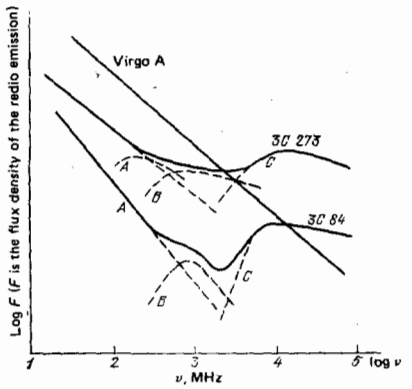

FIG. 1. Spectra of sources of cosmic radio emission: a giant elliptic galaxy, the radio source Virgo A, the quasar 3C 273, and a Seyfert galaxy, the radio source 3C 84. The broken curves show individual spectral components.[2]

As the accuracy of the measurements of the coordinates of the radio sources was increased, it became possible to identify objects having peculiar spectra with faint stars. It was assumed that these stars belong to our Galaxy, and therefore the sources with high-frequency excesses in the spectra would not constitute some new class of objects. The radio sources 3C 84, 3C 147, 3C 196, 3C 273, and 3C 286 were identified for the first time on photographic plates obtained at the Mount Wilson and Mount Palomar observatories.[3] (The designations in the Third Cambridge Catalog are given.) After the Sun, these were the first stars for which radio emission was detected. However, further investigations showed that these are far from being ordinary stars and are objects of a special class—quasistellar objects or quasars. For a long time, the spectral lines of the quasars could not be identified with the lines of known elements. It was realized subsequently that this is due to their large red shift, which reaches several tens of percent. Thus, the bright emission lines observed in the spectrum of the quasar 3C 273 could be identified with the Balmer series of hydrogen only under the assumption that they are shifted to the red by 16%. If this red shift is due to the cosmological distance to the objects, then quasars are at distances that reach several billion light years. But they must then radiate an unusually high power $\sim 10^{45}$ erg/sec. The emission of the source will last for ~10 000 years, and the total energy released by the quasar will be $\sim 10^{56}$ erg. For comparison, the nuclear energy released by complete transformation into helium of a mass if hydrogen equal to the solar mass is only $\sim 10^{52}$ erg; moreover, the process of transformation of hydrogen into helium would last $\sim 10^{10}$ years.[3]

As was established by Ginzburg and Shklovskiĭ, the radiation of the majority of cosmic sources is due to the synchrotron mechanism—the radiation of relativis-

 0038-5670/83/070612-22$01.80

tic electrons moving in a magnetic field. In particular, this found brilliant confirmation in the polarization of the radio emission of the sources.

The higher the energy E of the electron, the higher the frequencies it radiates, $\nu \sim H_\perp E^2$, but the more rapidly it loses its energy: $t \sim E^{-2} H^{-5/2}$. Thus, the high-frequency excesses in the spectra of the radio sources must be associated with sources of high-energy electrons, since the lifetime of these electrons is appreciably shorter than the lifetime of the object. The connection between the high-frequency excess and a source of electrons and their short lifetime indicates that the region of the emission must be compact, so that in view of the huge distances to the objects the emission region must have exceptionally small angular dimensions.

Further theoretical investigations of the synchrotron mechanism of radio emission[4,5] showed that the characteristic low-frequency "dips" of the high-frequency excesses are determined by the absorption of radiation by the relativistic electrons themselves (reabsorption) and are related to their angular dimensions[6]:

$$\varphi[\text{arcsec}] = 1.4 \cdot 10^{-2} F_0^{1/2} \nu_0^{-5/4} H^{1/4} (1+z)^{1/4},$$

where F_0 and ν_0 are the maximal flux density of the radio emission of the object and the frequency at the turning point of the spectrum (expressed in 10^{-26} W · m^{-2} · Hz^{-1} and GHz, respectively), H is the magnetic field intensity in oersteds, and z is the red shift. The magnetic field has little influence on the angular dimensions of the source; the magnetic field is usually $\leq 10^{-3}$ G.[7,9,10]

The high-frequency excesses of the strongest radio sources have $F_0 = 5-20$ Jy (1 Jy $= 10^{-26}$ W · m^{-2} · Hz^{-1}) and $\nu_0 = 10-40$ GHz. In this case, the expected angular dimensions of these sources must be $\varphi \leq 1$ marcsec. For sources for which the slope of the spectrum changes at meter or decimeter wavelengths, the angular dimensions must be $\varphi = 0''.1-0''.01$.

To determine the nature of the radio emission of the quasars, it was necessary to measure their angular dimensions. This cannot be done even with the most powerful modern optical telescopes, let alone radio telescopes. Radio waves are hundreds of thousands of times longer than optical waves, and to achieve the necessary angular resolution one would need an instrument of the size of the terrestrial sphere. It is for this reason that even the largest radio telescopes with bowls if diameters reaching tens of meters do not improve on the angular resolution of the unaided eye.

Significant successes were achieved by the development of the method of occulation. If the Moon occults a source, a diffraction pattern is formed at the limb, its form depending on the angular dimensions of the source (the distribution of the radio brightness); its time of occurrence depends on the relative position of the Moon and the investigated object.[11,12,65] The accuracy in the determination of the coordinates and the angular dimensions of sources at decimeter wavelengths reaches $\sim 1''$. In 1963–1964, one of the most interesting quasars, 3C 273, was occulted several times. Observations were made using large radio telescopes in Australia and in the Soviet Union at the Deep Space Communication Center in the Crimea.[11,13] The Australian scientists attached such importance to these results that the obtained traces were copied and sent for analysis in different aircraft. These observations made it possible to identify in the quasar two components—a nucleus (component B) and an extended ejection (component A). The diameter of the nucleus was found to be $\leq 1''$. It was the nucleus that was found to be responsible for the high-frequency excess, the ejection having an ordinary power-law spectrum (see Fig. 1); the spectral index of the ejection is $\alpha = 0.65$.[13] Subsequent optical investigations confirmed the presence of the ejection, which is at a distance of $19''.5$ from the nucleus and measures $2'' \times 10''$. It is oriented at angle 223°; at the position of component B, a $\sim 13^m$ star was discovered.[14]

Further improvement in the radio-astronomical methods made it possible to increase the angular resolution further. When radio waves propagate through an inhomogeneous ionized medium there is a focusing of the radiation, as a result of which a radio source, like stars in the optical range, scintillate. The magnitude of the scintillation depends on the relative angular dimensions of the radio source and the "lens." The larger the angular dimensions of the source, the smaller the amplitude of the scintillations. It is for this reason that the planets do not scintillate—their angular dimensions are appreciably greater than the dimensions of the inhomogeneities of the atmosphere. Thus, the interplanetary medium was found to be an "instrument" with high angular resolution.[22,23,82,84] Observations of the scintillation of quasars confirmed their small angular dimensions. At meter wavelengths, these were found to be $\sim 0''.1$, and at decimeter wavelengths $\leq 0''.04$.[15-21] Use of the interstellar medium made it possible to raise the angular resolution still further, to $10^{-6}-10^{-7}$ arcsec.[16,209] Thus, a connection was established between sources with high-frequency spectral excesses and small angular dimensions of the emission regions. It was then necessary to identify the sources of the high-energy particles.

The process of injection of the high-energy particles must be nonstationary, and one could therefore expect the high-frequency radio emission of the objects to be variable. Variability of the radio emission of objects with active nuclei was observed for the first time at centimeter wavelengths from the quasars 3C 345, 3C 273, and a number of other sources[26-27] and was studied in detail in Refs. 24, 25, and 28–30. It was found that the variability has a random nature and consists of individual outbursts of radio emission (Fig. 2).[7,28] The outbursts first appear at short and then at longer wavelengths. At the same time, the magnitude of the outbursts decreases and their duration increases. At sufficiently high frequencies (at millimeter wavelengths) the time of appearance of an outburst and its duration do not depend on the wavelength. Outbursts can appear fairly frequently and be superimposed on one another, as, for example, in the objects 3C 84, 3C 273, and 3C 345, or they may occur seldom, as in the object 3C 120.[31-38,125]

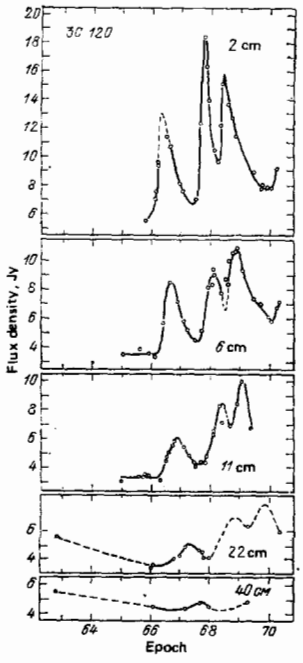

FIG. 2. Change in the radio emission of the Seyfert galaxy 3C 120 at different wavelengths.[28]

The characteristic time of variation of the radiation intensity of a quasar is about a month, but in individual cases the time of an outburst does not exceed a few days. Just as rapid variations occur in the optical range.[31,36,37]

The dimensions of a radio source cannot exceed the distance traversed by the radiation during the time of existence Δt of the outburst, i.e., $l \leq c\Delta t$. And this do means that the angular dimensions of rapidly varying sources do not exceed $\varphi \approx 0.002$–0.2.[38]

The radiation of objects with active nuclei is linearly polarized, which indicates that it has a synchrotron origin. The magnitude of the polarization and its position angle vary.[31,36,37]

The astronomical objects with active nuclei can be divided into quasars, BL Lacertae objects, Seyfert galaxies, and ratio galaxies with active nuclei. In a number of cases this division can be somewhat arbitrary. Some objects do not have identifications in the optical range. This could be due to the fact that the regions are obscured by dust or that they have little optical radiation. Clear differences in the radio variability of these objects are not observed, but the outbursts of quasars and BL Lacertae objects are more intense, corresponding to changes in radiated power of ~10^{45} erg/sec yr, whereas the outbursts in the nuclei of radio galaxies are appreciably weaker, ~10^{42} erg/sec yr.[7] In recent years extended regions around a number of quasars have been discovered and identified with galaxies. Thus, classical quasars such as 3C 273, 3C 48, and 3C 37, 43 are the nuclei of galaxies.[40,142] It is possible that the remaining objects are galaxies, the only difference being in the activity of the nuclei.

The radio emission of the nuclei of the objects and the individual outbursts can be described fairly well by the synchrotron mechanism. In particular, the observed radiation of the regions of the outbursts can be represented as adiabatically expanding clouds of relativistic particles whose magnetic flux is conserved. The clouds of particles are ejected from the nuclei of the objects as a result of active processes.[7,41-47]

In the adiabatic model, the ejected cloud initially has large optical thickness $\tau > 1$, and the flux density of its radio emission increases as $F \sim t^3$. This continues until the cloud becomes optically thin, $\tau < 1$. At this time, the flux begins to fall as $F \sim t^{-2\gamma}$, where γ is the exponent of the energy spectrum of the electrons. In the special case when the energy distribution of the electrons is represented by a power law, the spectrum also has a power-law nature, $F \sim \nu^{\alpha}$, and the spectral index is $\alpha = -(\gamma - 1)/2$.

The optical thickness of a cloud of relativistic particles depends on the frequency ν, and the maximal flux density of the radio emission is at the frequency $F_{max} = \nu^{(7\gamma+3)/(4\gamma+6)}$. At frequencies $\nu < \nu_{max}$, the optical thickness is $\tau > 1$, and the flux density of the radio radiation depends on the frequency as $F \sim \nu^{2.5}$, while at frequencies $\nu > \nu_{max}$, $\tau < 1$ and $F \sim \nu^{\alpha}$. As the cloud expands, the frequency ν_{max} is shifted to lower frequencies as $\sim t^{-(4\alpha+5)/(\alpha+2.5)}$.

At high frequencies $\nu > \nu_{max}$, the region of the radio outburst is transparent, and the variation of the flux density of the radiation occurs simultaneously at all frequencies and reflects the rate of generation of the high-energy particles or their "disappearance" due to synchrotron loss and inverse Compton scattering.[48,49] The observed radiation will be determined by the total number of particles, their energy distribution, and the magnetic field H. In this connection, observations at high frequencies are the most effective and make it possible to follow the evolution of nonstationary phenomena in the early stage of development of a outburst.

However, observations at frequencies $\nu < \nu_{max}$, where the source has $\tau > 1$, make it possible to determine the magnetic field intensity H. In this part of the spectrum

$$H \approx 0.5 \cdot 10^{20} T_b^{-2} \nu \text{ [Oe]},$$

where ν is expressed in gigahertz and T_b in degrees Kelvin.

The maximal brightness temperature of an optically thick source of synchrotron radiation is limited by inverse Compton scattering.[7,49] For a homogeneous, isotropically radiating source the ratio of the power L_C of the inverse Compton scattering to the power L_s of the synchrotron radiation is

$$\frac{L_C}{L_s} \approx \frac{1}{2}\left(\frac{T_{max}}{10^{12}}\right)^5 \nu_0 \left[1 + \frac{1}{2}\left(\frac{T_{max}}{10^{12}}\right)^5 \nu_0\right].$$

It can be seen from this expression that for $T \geq 10^{12}$ °K the Compton losses increase sharply.

$$\frac{L_C}{L_s} \sim \left(\frac{T_{max}}{10^{12}}\right)^{10}.$$

The exact value of T_{max} corresponding to $L_C/L_s = 1$ depends on the geometry of the source, the energy distribution of the electrons, and the magnetic field intensity. However, T_{max} cannot differ strongly from $T_b = 10^{12}$ °K at all wavelengths. The limiting value of the magnetic field in this case is $H \approx 10^{-4}\nu$.

If a compact source expands with conservation of the magnetic flux, then T_{max} depends on its radius as $T_{max} \sim \rho^{-(\gamma-1)/(\gamma+4)}$, and in the case of a power-law energy distribution of the electrons its spectral index is $\alpha = -(\gamma-1)/2$. For $\gamma = 1$, T_{max} is almost independent of ρ.

As follows from the variations in time, the angular dimensions of the regions of the outbursts are ~0.01 marcsec, and the flux density of the radio emission reaches ~10 Jy, which corresponds to the unusually high brightness temperature $T_b \approx 10^{13}$ °K and clearly exceeds the maximally permitted values. Another, no less complicated question is the problem of the enormous energy of the nuclei and the mechanism of its transformation into the energy of the magnetic field and the relativistic particles. To find answers to these questions, it was necessary to measure the detailed structure of the compact central regions of the radio sources, their cores, to identify individual components, and to follow their evolution. Initially, it seemed that this problem could never be solved, its resolution requiring an instrument with an angular resolution <1 marcsec. Radio telescopes with such resolution would have to have global dimensions.

The development of quantum radio physics, computational techniques, and antenna systems created the prerequisites for the solution of this problem. The foundations of a new method were laid—radio interferometry with very long baselines (VLBI).[50] This method opens a new epoch in astronomy—compact cosmic objects such as the nuclei of quasars and radio galaxies and the regions of formation of stars and planetary systems became accessible to investigation. The best angular resolution that can be obtained under terrestrial conditions, ≤100 μarcsec, has now been achieved.[51,52,97,98] However, the dimensions of the Earth are not a fundamental limit and present only certain technical difficulties. Modern space capabilities already make it possible to carry a radio telescope into orbit around the Earth.[53,54,181]

2. VLBI

The method of radio interferometry with very long baselines consists of receiving signals from the investigated cosmic object (or any other source of radio signals) with widely spaced antennas, their transformation to the videofrequency band, and magnetic recording. The coherent transformation of the signals and the synchronization of the recording at the two points of observation are made by means of high-stability oscillators of atomic type. Usually, frequency standards of hydrogen or rubidium type are used. The former are more stable: $\leq 10^{-14}$ over a time of ~10^3 sec. The traces on the magnetic tapes are transported to the computational center and are simultaneously analyzed

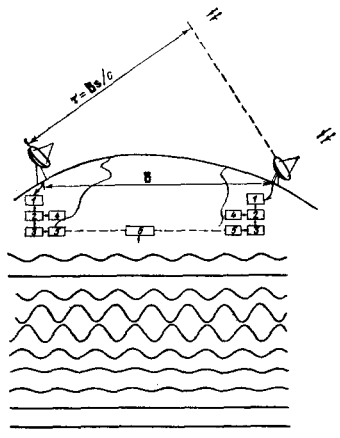

FIG. 3. Radio interferometer with very long baseline. 1) High-frequency amplifier, 2) signal frequency converter, 3) video-frequency band amplifier, 4) atomic frequency standard, 5) magnetic recorder. The baseline of the interferometer is B. At the bottom, we show the interference fringes on the processor display 6 obtained from the quasar 3C 273 at wavelength 1.35 cm. Crimea-Effelsberg baseline.

with specialized computers. From the data of cross-correlation analysis the distribution of the radio brightness of the object is determined. Thus, the elements of the interferometer are not directly connected, and the distance between them can be made arbitrarily great (Fig. 3).

In contrast to an ordinary mirror telescope (instrument with filled aperture), the angular resolution of the interferometer is determined by the distance between the antennas, and not their diameters. Only the sensitivity of the interferometer depends on the diameter of the antennas, and it is only in this sense that their diameters limit the angular resolution.

A VLB radio interferometer is analogous to a Michelson interferometer in the optical range. In contrast to a radio telescope with continuous aperture, it does not detect the brightness of a particular area (point) of the image of the object, $T_b(x, y)$, but rather one of the spatial harmonics of its image—a Fourier component of the distribution of the radio brightness,

$$A(u, v) = \int T_b(x, y) \exp\left[-j \cdot 2\pi (ux + vy)\right] dx\, dy,$$

where x and y are coordinates on the plane of the celestial sphere, and u and v are the spatial frequencies.

The spatial frequency measured by the interferometer (the response of the interferometer) is determined by its baseline B, i.e., the distance between the antennas and its orientation. These frequencies are

$$u = \frac{B}{\lambda} \cos\delta_B \sin(T_S - T_B),$$

$$v = \frac{B}{\lambda} [\sin\delta_B \cos\delta_S - \cos\delta_B \sin\delta_S \cos(T_S - T_B)],$$

where δ_B, δ_S are the declinations and T_B, T_S the hour angles of the baseline and the source, respectively. The vector of the baseline describes on the u, v frequency plane the ellipse

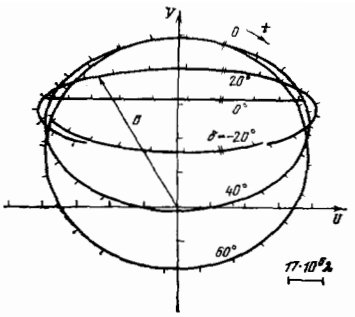

FIG. 4. Projections of the baseline of the Crimea-Pushchino interferometer at wavelength 1.35 cm for different declinations δ as a function of the hour angle t. This shows the covering of the u, v plane.

$$\frac{u^2}{a^2}-\frac{(v-v_0)^2}{b^2}=1,$$

whose semimajor axes are equal to

$$a=\frac{B}{\lambda}\cos\delta_B,$$

$$b=\frac{B}{\lambda}\sin\delta_B\cos\delta_B,$$

and the displacement along the v axis is

$$v_0=\frac{B}{\lambda}\sin\delta_B\cos\delta_B,$$

where B is the projection of the baseline onto the equatorial plane.

Figure 4 shows the projections of the baseline of the Simeiz (Crimea)-Pushchino interferometer for declinations $\delta=-20-60°$.[153] The projections are given in wavelengths ($\lambda=1.35$ cm). The marks indicate the hour angles. Thus, the ellipse reflects the frequencies that can be measured by the given interferometer.

Observing the source of different hour angles, one can measure a certain region of harmonics of the Fourier distribution of the brightness of the investigated object. The distribution of the radio brightness of the object is obtained from the spatial harmonics by inverse Fourier transformation:

$$T(x,\ y)=\int A(u,\ v)\exp[j\cdot 2\pi(ux+vy)]\,du\,dv.$$

However, for this all the frequencies and their phases must be measured, i.e., observations of the object must be made with radio interferometers with bases of different lengths and orientations, i.e., one must obtain a complete covering of the u, v plane, which is equivalent to synthesizing an antenna whose aperture is equal to the baseline base of maximal length. In practice, the investigations into the structure of radio sources by VLBI are made with existing radio telescopes, and accordingly the vectors of the baseline are determined by their relative positions. In addition, measurements of the phases of the harmonics present certain difficulties. For this reason, the distribution of the radio brightness is not determined by inverse Fourier transformation but in a model approximation—distributions of radio brightness are specified, their spatial frequencies are calculated, and then the least-squares method is used to determine the minimal deviation of the calculated and measured values of the amplitudes of the Fourier harmonics. As a rule, one uses the simplest models with a limited number of components with Gaussian brightness distribution. In the models, one calculates the relative position of the components, their dimensions, ellipticity, position angle, and flux density of the radio radiation.[55-58] The relative position and size of the components are determined with an accuracy up to fractions of the width of an interference fringe. The accuracy depends on the sensitivity of the telescopes.

In the meanwhile, improved methods of calculating the models have been developed, these making it possible to determine the brightness distribution of individual points of the source. A grid of point sources is specified on some area with a definite step. The flux densities of each of them is chosen such that the spectrum of the spatial frequencies of the set of sources has minimal deviation from the measured values. The mosaic image is then smoothed by a Gaussian function and "cleaned"—it is corrected for the diagram of the interference system.[58-64] Figure 12 (see below) shows a chart of the nucleus of the Seyfert galaxy NGC 1275 obtained by this method.[64]

Further improvement in the methods of image construction involve the use of the so-called method of closure phases. It was first used for radio interferometers with short baselines.[66] It is a form of differential method. In observations with three antennas forming three radio interferometers, the phases determined by instrumental effects, including instability of the heterodynes and the influence of the atmosphere and the ionosphere, occur in the different interferometers with opposite signs and cancel each other. Thus, the spatial frequencies obtained using three interferometers can be mutually matched in phase, which appreciably raises the accuracy of the modeling.[63] The method of closure phases reproduces with high accuracy an image of the object, but it does not eliminate the absolute error in the determination of the position of the source on the celestial sphere. At the present time, observations of radio sources are made with a large number of radio telescopes simultaneously, and the results are analyzed in "triplets," which ensures mutual matching of the spatial harmonics of the image of the object.

A high accuracy of measurement is also attained when a reference detail is used. This form of differential method is especially effective if a point source is present within the limits of visibility of the directional diagram of the radio telescope. Such a source can be one of the details of the investigated object. It is for this reason that one can measure with high accuracy the relative positions of the components of a radio source. This method is widely used for measurements of the fine structure of maser sources, to study their dynamics, and also the structure of quasars with comparatively simple structure.[67,57,68] In a number of cases, the accuracy reaches 50 μarcsec.[69,188]

3. RADIO INTERFEROMETERS WITH VERY LONG BASELINES

Investigations into the fine structure of radio sources by VLBI have become one of the most important directions of modern radio astronomy. Observations are made in the entire spectrum of radio wavelengths from meter to millimeter waves inclusively.[51,64,65,81,88,126]

All the largest radio telescopes of the world are used in the measurements. The choice of the wavelength is determined by a number of factors: 1) the angular resolution, 2) the conditions of visibility of the fine structure of the objects, 3) the technical possibilities of the instruments.[38,70]

The angular resolution of a radio interferometer is $\Delta\varphi \sim \lambda/B$; there is therefore a natural desire to shorten the wavelength and increase the baseline B.

The conditions of visibility of compact sources are determined by the transparency of the ionized medium surrounding the nuclei of the quasars and radio galaxies; the transparency is proportional to λ^{-2}. Therefore, the observations of the deep layers of nuclei must be made at the shortest possible wavelengths. The increase in the flux density of the radio emission of compact, optically thick components right down to the millimeter wavelength range facilitates this.

The maximum of the radiation of relatively "old" components is at wavelengths in the centimeter–decimeter range.

The technical possibilities of modern large radio telescopes permit reliable operation in the complete range of centimeter wavelengths. These possibilities are determined by the accuracy in the construction of the mirrors and the retention of their shape at different angles of elevation, the accuracy of guiding the antenna, the sensitivity of the instruments, the stability of the phase of the apparatus, including the heterodyne systems, and, finally, the transparency of the atmosphere.

At millimeter wavelengths, the atmosphere seriously limits the possibilities of interferometry on account of not only absorption of the signal and its own radiation but also on account of phase instability. Therefore, millimeter-range instruments are built high in mountains. The total electric path length in the atmosphere varies as cosec h, where h is the angle of elevation, and reaches 2 m in the direction of the zenith.[71] For decimeter and longer waves, the limiting factor may be the ionosphere; its electric length at wavelength 18 cm is approximately equal to the length of the troposphere and is proportional to $\sim\lambda^2$.

The next restricting factors are the interplanetary and interstellar media. They are inhomogeneous and limit the angular resolution, smearing the apparent angular dimensions of the sources, i.e., they play a negative part, in contrast to the scintillation method.

As follows from the experimental data, the scattering angle in seconds of arc is

$$\theta_{scat} \approx 10^{-6}\,\lambda^2\,|\sin b\,|^{-0.5},$$

where λ is expressed in centimeters. At low galactic latitudes $|b| < 10°$, the scattering increases sharply because of the influence of the matter concentrated in the arms of the Galaxy and gas-dust complexes. For wavelengths ~1 cm, the scattering angle is $\theta_{scat} \geq 10^{-6}$ sec, whereas at wavelength 1 m it is $\geq 10^{-2}$ sec. On the basis of this, the limiting length of the baseline in kilometers is

$$B < 10^6\,|\sin b\,|^{0.5}\,\lambda^{-1}.$$

At meter wavelengths, the baselines are shorter than the Earth's diameter, whereas at short centimeter wavelengths the baselines may reach $\sim 10^5$ km. However, the limiting factor in this case may be the sensitivity, which depends on the time T of coherent accumulation of signals, the noise temperatures T_{n1} and T_{n2} of the systems, the effective areas A_1 and A_2 of the antennas, and the band Δf of the received signal. The limiting length of the baseline in kilometers in this case is

$$B < 10^{-4} T_b^{0.5}\,(T_{n1}T_{n2})^{-0.25}\,(A_1A_2\Delta f T)^{0.25},$$

where T_b is the brightness temperature of the investigated source. In the limiting case, the brightness temperatures of the components of objects with active nuclei is $T_b \approx 10^{12}$ °K, and for maser sources emitting water vapor lines it is $T_b \approx 10^{16}$ °K, but the signal band is determined by the width of the line and is equal to ~50 kHz. The limiting baseline for a space radio telescope of diameter 30 m with noise temperature $T_a \approx 50$ °K of the system and terrestrial diameter 100 m with noise temperature 50 °K of the system is $B < 10^5$ km; here, the signal reception band has been taken to be 2 MHz, and the time of coherent accumulation 100 sec.

The optimal radio wavelengths for radio astronomical investigations are 1.35, 2.8, 6, and 18 cm.

Observations of radio sources are currently made with a large radio interference network, which includes virtually all the radio telescopes in the world (Table I).

Table I gives the location of the antennas, their diameters, their coordinates X, Y, Z, wavelengths, and type of employed frequency standard (H for hydrogen and Rb for rubidium).

TABLE I.

Location	$\varnothing$, m		λ, cm	X	Y	Z
				10^{-3} km		
Crimea	22	H	1.35; 18	3.8	−2.6	4.4
Effelsberg	100	H	1.35; 2.8; 6; 18	4.0	−0.5	4.9
Onsala	20/26	H	1.35; 2.8; 6; 18	3.4	−0.7	5.3
Dwingeloo	26	H	6; 18	3.8	−0.4	5.1
Jodrell Bank	26/75	Rb	6; 18	3.8	−0.2	5.1
Tidbinbilla	64/26	H	1.35; 3.75; 13; 2	4.4	2.7	3.7
Goldstone	*64/26*	*H*	*2; 3,75; 13*	−2.4	4.7	3.7
Madrid	64	H	2; 3,75; 13	4.9	0.4	4.1
Green Bank	43	H	1.35; 2; 2,8; 6; 18	0.8	4.9	3.9
Maryland Point	26	H	1.35; 2.8; 6; 18	1.1	4.9	3.9
Fort Davis	26	H	2.8; 6; 18	1.3	5.3	3.2
Owens Valley	40	H	1.36; 2.8; 6; 18	−2.4	4.5	3.8
New Mexico	26	Rb	1.35; 2.8; 6; 18			
Arecibo	300	Rb	6; 18	2.4	5.6	2.0
Hat Creek	26	*Rb*	*1.35; 2.8; 6; 18*	−2.5	4.1	4.1
Haystack	37	H	1.35; 2.8; 3,7; 6; 18	1.5	4.4	4.3
Algonquin	47	H	2.8; 3.7; 6; 18	0.9	4.3	4.6
Johannesburg	26	Rb	3.7; 18	5.1	−2.7	−2.8
Vermilion River	37	Rb	2.8; 6; 18	0.2	4.9	4.1

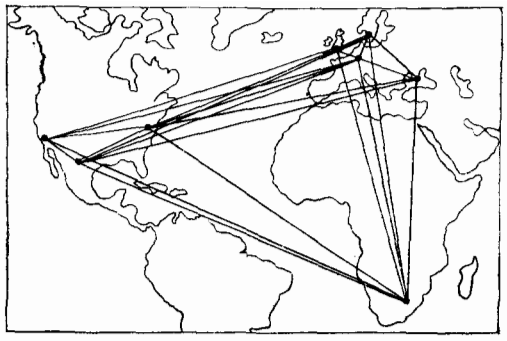

FIG. 5. Global radio interferometer network at wavelength 18 cm.

The angular resolution of the network at wavelength 1.3 cm reaches the limit ~50 μarcsec under terrestrial conditions. No other physical instrument has such a high resolution. This resolution corresponds to the angle subtended by the orbit of an electron in the hydrogen atom at a distance of 20 cm. The use of a large number of radio sources ensures that the measurements have a high information content (the number of baselines formed from m instruments is $m(m-1)/2$) and good covering of the u, v plane. Figure 5 shows the radio interference network used in 1980–1981 to study the structure of quasars.[178]

4. STRUCTURE OF COMPACT EXTRAGALACTIC SOURCES

a) The Seyfert galaxy 3C 120

The Seyfert galaxy 3C 120 is one of the most interesting objects. There is a clear high-frequency excess in its spectrum (Fig. 6). The red shift of the galaxy is $z=0.0323$, and the distance to it, under the assumption that $H=75$ km · sec^{-1} · Mpc^{-1}, is 130 Mpc. Unusually active processes, accompanied by intense outbursts of radio emission, occur in the nucleus of this galaxy. Figure 2 shows the change in the flux density of the radio emission at different wavelengths.[7,28] The outburst at the end of 1967 at wavelength 2 cm reached 12 Jy, which exceeded by a factor 2 the level of the "quiescent" radiation. At longer wavelengths, the outbursts are delayed, and their intensity decreases. The optical radiation of the nucleus is also variable.[32,39,73]

The first observations using VLB radio interferometers at wavelengths in the 3-cm range established a complicated structure of 3C 120.[72,74–77,78,81,91,92]

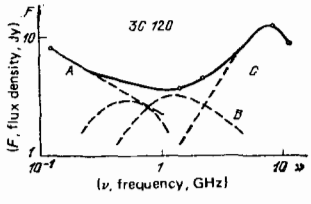

FIG. 6. Spectrum of the source 3C 120. The broken curves show the individual spectral details.[7]

TABLE II.

Time	Two components					Ring (diameter), marcsec
	Distance, marcsec	Diameter, marcsec	Angle, deg	Flux		
				short wavelength	total	
28.02.71	0.98	0.5	95	6.5	9.2	1.44
25.06.71	1.3	0.7	85	4.5	7.6	1.8
03.11.71	1.7	1.3	85	7.0	10.7	2.5
04.72	$\leqslant 0.4$	$\leqslant 0.4$	—	—	9.8	—
06.06.72	—	—	—	—	9.4	—
08.72	$\leqslant 0.4$	$\leqslant 0.4$	—	—	13.1	—
29.08.72	$\leqslant 0.3$	$\leqslant 0.3$	—	—	13.4	—
10.72	0.6	$\leqslant 0.4$	~60	—	15.3	—
07.11.72	0.99	0	65	12.0	15.8	0.74; 10
05.02.73	1.0	0	65	10.4	14.4	1.17
15.03.73	1.1	0.9	62	8.0	19.4	—
		0.6		7.2		
30.03.73	1.11	—	65	10.2	16.5	1.65
17.05.73	1.23	—	65	7.8	14.7	1.98
15.06.73	1.3	0.9	65	2.9	13.6	—
		0.8		7.2		
22.02.74	2.8	0.8	65	2.2	10.1	—
		0.9		3.3		

Further investigations revealed a significant change even during a few months.[70,76,84,89,99] The results of observations in the period February–November 1971 were represented in the form of two separated components with position angle equal to 85–90°, or in the form of a ring. These models are given in Table II. The diameter of the ring increased during 1971 from 1.4 to 2.5 marcsec, while in the case of two components their separation increased from 1 marcsec to 1.7, the diameters increasing from $\leqslant 0.5$ to 1.3 marcsec. Bearing in mind the distance to the object, the observed changes took place with superluminal velocity. In the first half of 1971, the separation and expansion of the components occurred at the veloities $1.6c$ and $1.2c$, and in the second half at $2.1c$ and $3.1c$, respectively. Further observations confirmed this structure. Figure 7 shows the change in the relative position of the two components.[90] The data obtained at different wavelengths are generalized in this figure. The results lie on two straight lines, reflecting two phases of activity of the object. The observed difference between the positions of the components at the wavelengths 2.8 and 3.8 cm at 1974.5 was explained by the spectral features of the new pair of components. Figure 8 shows the change in the flux density of the radio emission during this period, the observed changes belonging to different outbursts. The main radiation of the source in 1972.5–1974.5 was determined by one pair of components moving apart with velocity ~$5c$, while in the period 1974.5–1976 it was determined by a new pair with velocity $8c$. At 1974.5, the new pair was seen at

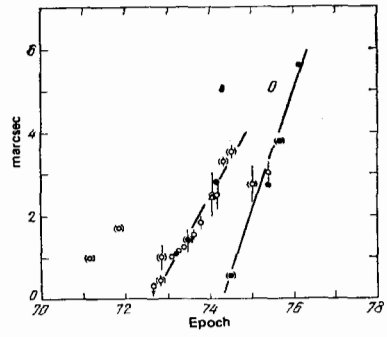

FIG. 7. Change in the distance between the two components in the source 3C 120.[90]

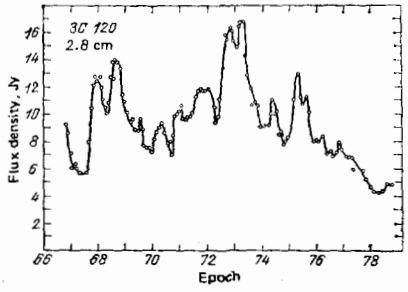

FIG. 8. Change in the flux density of the radio emission of the source 3C 120 at wavelength 2.8 cm.

the wavelength 2.8 cm, but its radiation was still insufficiently great at the wavelength 3.8 cm, which explains the observed difference.

Investigations of the structure of 3C 120 using a multielement interferometer with five radio telescopes during 1972–1974 confirmed the two-component model.[86,87] At the same time, one cannot rule out a model whose components keep their position but change their brightness; at the same time, the position angle remains the same.[100]

Observations at wavelengths 2.8 and 6 cm during 1976–1977 with five radio telescopes confirmed that the position angle of the object remained the same. During this period, its activity decreased (see Fig. 8), and its extension increased. Analysis yielded a hybrid chart containing three components separated by ~1 marcsec from one another (Fig. 9a).[94,184] It can be interpreted as a bright nucleus and components ejected from it in the direction with position angle −108°. For greater clarity, Fig. 9b shows the distribution of the brightness along this direction. The nucleus and the component nearest to it have flat spectra, while the far component has a power-law spectrum with spectral index −1. The velocity of the ejected components is 1.85 marcsec per year or $5c$ assuming $H=55$ km · sec^{-1} · Mpc^{-1}, $q_0=0.05$, and $z=0.033$.

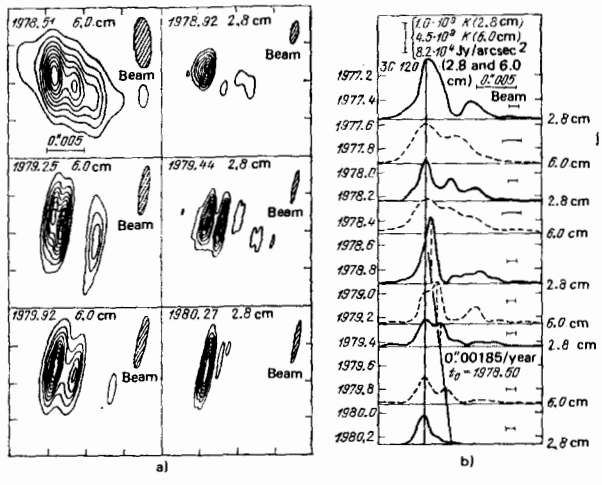

FIG. 9. Distribution of the radio brightness in the source 3C 120 at wavelengths 2.8 and 6 cm (a), and distributions of the radio brightness along the major axis of the source (b).[184]

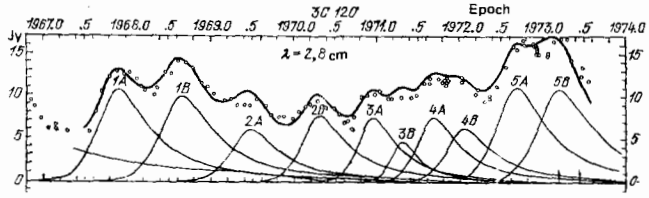

FIG. 10. Change in the flux density of the radio emission of the source 3C 120 at the wavelength 2.8 cm and the corresponding outbursts of radio emission.[33]

The complicated three- or even four-component collinear structure in the period 1976.73 (at frequency 10 650 MHz) and at 1977.41 (at frequency 5010 MHz) was confirmed in Refs. 93 and 95. A general decrease of the radiation region was noted after 1976. It should be pointed out that the considered model with superluminal separation of the components is not unique, and one can construct an image of the source with stationary position of the components but variable brightness.[93-95]

The observed variations in the brightness of the components of 3C 120, their relative position, and the variability of the radio emission are fairly well described by the model considered in Ref. 44. The variability of the radio emission is represented by the change in the emission of two plasmoids (clouds of relativistic particles) ejected from the nuleus in two opposite directions. Their radiation is determined by the synchrotron mechanism. The velocity of motion and the velocity of expansion of the components are near the velocity of light.[33] The outbursts of radio emission are repeated approximately every 1–2 years (Fig. 10). As follows from the model of Ref. 44, component A, which moves in a direction close to the direction to the observer, has a greater intensity than component B, which moves in the opposite direction. The maximum of the radiation of component B is observed later than that of A. The figure shows pairs of outbursts corresponding to the experimental data.

The relative intensity of the radiation of the components is

$$\frac{S_{A\,max}}{S_{B\,max}}=\left(\frac{1+\beta_{sep}\cos\theta}{1-\beta_{sep}\cos\theta}\right)^{1.875},$$

where θ is the angle between the direction of motion of the components and the direction to the observer.

As is shown in Ref. 101, the expansion velocity of an optically thick spherical cloud, $v_{exp}=\beta_{exp}c$, will appear to be $2v_{exp}(1-\beta_{exp}^2)^{-0.5}$ for an external observer. On the basis of the experimental data, the expansion velocity of optically thick components will be $\beta_{exp}=0.63$ (Table III). In the case of components, their separation velocity for an external observer will appear to be

$$v_{arr.}=\frac{2v_{sep}\sin\theta}{1-\beta_{sep}^2\cos^2\theta},$$

where v_{sep} is the velocity with which the components move.

It follows from the relative intensity of the radiation of the two components and their apparent separation

TABLE III.

Outburst	Expansion velocity, c	Separation velocity, c	β_{exp}
1B	1.7		0.65
3A	2.9	$\leqslant 2.3$	0.82
3B			
4A	$\geqslant 3.1$	$\leqslant 4.1$	$\geqslant 0.84$
4B	$\leqslant 0.8$		$\leqslant 0.37$
5A	$\leqslant 1.0$	1,6	$\leqslant 0.45$
5B			

velocity that $\theta = 60-80°$, and the separation velocity lies in the interval $\beta_{sep} = 0.6-0.8$.[33]

The high brightness temperature of the components, even exceeding the Compton limit, can also be explained in the framework of this model. In the case of motion of components with velocity near the velocity of light their radiation becomes directed.

b) The Seyfert galaxy NGC 1275

The Seyfert galaxy NGC 1275, the ratio source 3C 84, is a powerful source of radio radiation in the centimeter wavelength range. The red shift of the galaxy is $z = 0.0176$. The distance to it is 110 Mpc, and 1 marcsec corresponds to 0.55 pc. According to one theory, we have here colliding galaxies; according to another, an exploding galaxy.[108,109]

The object contains a system of filaments oriented at the angles ~60° and -10°. The extension of the filaments reaches ~100 kpc. It is assumed that the system of filaments belongs to a galaxy of late E type or SO type.[110] The velocity of the filaments and the nucleus of the galaxy is ~5200 km/sec. The spectral lines emitted by the nucleus of the galaxy are doubled. The doubling corresponds to a relative velocity ~600 km/sec of the emitting regions.[111] In front of the central part of the galaxy there is an absorbing medium, extended in the direction ~60°, and dense, compact bunches of matter that emit bright emission lines. According to the observational data, the angular dimensions of the absorption region in the neutral hydrogen line are 5×8 marcsec. There is a predominance of absorption in its eastern part, where the number of neutral hydrogen particles on the line of sight reaches 6×10^{20} cm^{-2}.[112] This system is identified with an intruding galaxy. Its velocity differs from the velocity of the filaments and is ~8200 km/sec.

At decimeter-meter wavelengths, the radio source 3C 84 (Perseus A) has diameter 5′ and is identified with NGC 1275 (Fig. 11).[9,105,106,113] It is one of the first radio sources in which a high-frequency excess in the spectrum was discovered (see Fig. 1).[28,114,115] It follows directly from the spectrum that besides the extended halo, which has an ordinary power-law spectrum, it must have a compact nucleus—a source of relativistic particles whose synchrotron radiation determines the high-frequency excess. Its angular dimensions must be ≤1 marcsec.

Variability of the radio emission of the source was observed and investigated in a wide range of wavelengths.[24,27,28] The currently observed excess radiation belongs to an active phase that began in the middle of the fifties. Since then, the flux density of the radio radiation has systematically increased.[117] The variation is irregular in nature and is associated with definite phases of enhanced activity of the nucleus. Each phase corresponds to a group of outbursts of radio emission, which occurred, for example, in 1969–1973 and 1974–1979. The outbursts are repeated fairly frequently and are superimposed on one another. The characteristic time of growth of an outburst is 1–1.5 yr. and the duration is 2–3 yr, the spectral index $\alpha = -0.25$.[113] The diameter of the region of emission of an outburst is, on the basis of its duration, ≤0.3 pc.

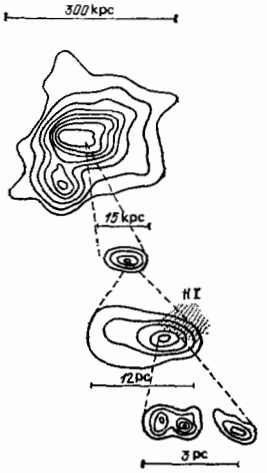

FIG. 11. Distribution of the radio brightness of the source 3C 84 at different "magnifications." The hatched part is the neutral hydrogen region.

Observations with VLB radio interferometers established a complicated structure of the central region of the object. At wavelength 75 cm, two components, separated by 37 marcsec in the direction with position angle -5°, were found.[118] Their diameters are 7.8 msec, and the brightness temperature is $T_b = 10^{11}$ °K. The emission of these components corresponds to the spectral detail B in Fig. 1. These components become optically thin at frequencies above 1 GHz. At wavelengths 6–21 cm one can separate emission of a central component, measuring ~3 marcsec, with brightness temperature $T_b \approx 10^{11}$ °K, and a surrounding extended structure measuring ~15 marcsec with $T_b \approx 10^{10}$ °K.[55,72,73,77,78,103-105,112]

Further detailed investigations of 3C 84 using multielement interferometers in the 3-cm wavelength range revealed a three-component structure oriented in the direction -9° with components measuring ~0.3 marcsec with brightness temperature $T_b \approx 5\times10^{11}$ °K and separated by ~3 marcsec.[57,63,97,87,103] Comparison of these data show that from 1971.5 to 1972 the distances between the components changed, the separation velocity being ~5c.

Improvement in the methods of analysis and more accurate measurements at 2.8 cm established a compli-

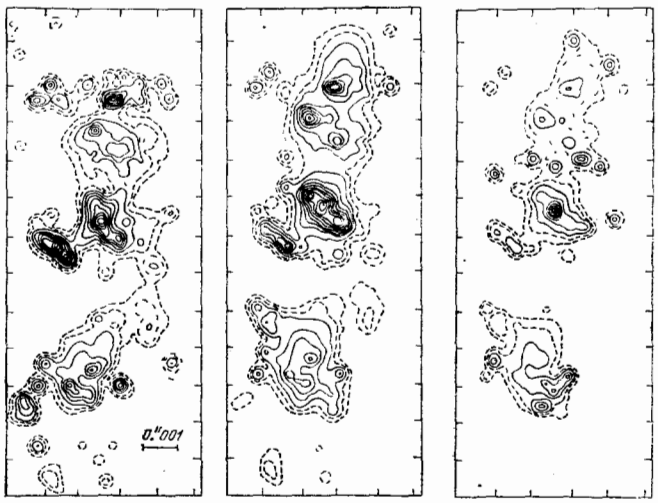

FIG. 12. Distribution of the radio brightness in the source 3C 84 at wavelength 1.35 cm during 1976.5–1977.9.[133]

cated structure of the central region of the source. Overall, it repeats the three-component structure.[107] It was found that evolution of the source is associated solely with a change in the brightness of the components, their position hardly changing (Fig. 12).[120,133] The upper limit of the velocity is $\leqslant 0.05c$.

In 1976, regular investigations with a global radio interference network were begun at 1.35 cm wavelength.[133] The angular resolution reached $\leqslant 100$ μarcsec. It was found that the nucleus consists of two systems—an eastern and a western. They are parallel and contain three groups of components—a northern, a central, and a southern (Fig. 13).[69,133] The distance between the systems is 0.7 pc, and the position angle −8°. The relative position of the components corresponds to the position at the wavelength 2.8 cm, but their brightnesses are very different, especially in the case of the eastern system. In Fig. 13, we show the

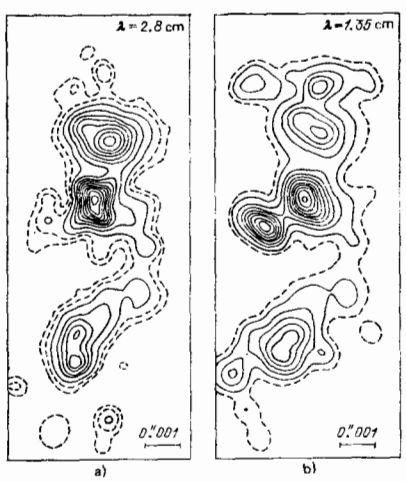

FIG. 13. Distribution of the radio brightness in the source 3C 84. a) At wavelength 2.8 cm in 1974.5, b) at wavelength 1.35 cm in 1976. The angular resolution in the two cases is approximately the same.[69]

brightness distributions of the nucleus of 3C 84 at the two wavelengths with the same angular resolution for greater clarity. The relative position of the individual components is preserved during the considered period, and only their brightness changes. At the end of the period, the brightness of the details of the eastern system decreased appreciably. At the same time, the brightness of the nucleus of the western system increased (see Fig. 12). The emission of the components of the eastern system still continued to decrease later.[210]

The central nuclei, in their turn, have a complicated structure with orientation angle different from the orientation of the object as a whole. The diameters of the components are $\leqslant 0.2$ marcsec, and the distance between them ~0.5 marcsec.

The northern and southern groups of components of both systems are at distance 3–4 marcsec from the nuclei, their angular diameters are 0.2–0.5 marcsec, and the brightness temperatures are on the average $\sim 10^{11}$ °K.

In 1976, the spectral index of the eastern system was $\alpha = 4.3$–4.5, which differs appreciably from the spectral index of an optically thick source of synchrotron radiation ($\alpha = 2.5$). The observed difference can be explained by the absorption of the synchrotron radiation of this region by an ionized medium. The existence of such a medium also follows from the optical observations.[36,37] The density of the ionized medium is directly related to the activity of the nucleus, which is indicated by the variability in the lines and also by the polarization of the radiation. The electron density of the ionized medium of the eastern system varies with the distance from the nucleus as $n_e \approx 4 \times 10^{45} L^{-2.3 \pm 0.5}$, where L is expressed in centimeters. At the same time, the magnetic field intensity decreases more slowly: $H \approx 10^8 L^{-0.5}$ Oe.[69]

The magnetic field intensity in the compact components reaches ~0.5 Oe, and in the region of optical emission 1–100 Oe.[36,37,111]

The electron density of the ionized medium surrounding the western system is significantly lower, $(1.7$–$5) \times 10^3$ cm^{-3}, and has an influence only at wavelengths in the decimeter range.[188,210]

The observed complicated distribution of the radio brightness of the central region of the galaxy, the persistence of the relative position of the compact components, and the change of their brightness can be explained by the structure of the magnetic field and the change in the filling of the magnetic tubes of force with relativistic particles. Each of the nuclei is surrounded by spiral magnetic fields observed edge-on. The planes of the spirals are parallel to each other. The position angle of the axes of rotation of the nuclei relative to the plane of the spirals is ~45°. Relativistic electrons ejected from the nuclei move along the magnetic lines of force, and the observer sees bright regions in the tangential directions, where the number of electrons on the line of sight is maximal. The diameters of these regions correspond to the transverse dimension

of the arm, and the structure of the magnetic field determines the fine structure of each of the components. A change in the number of electrons or their de-excitation leads to a change in the brightness of the components, but does not change their relative position. The direct emergence of the particles from the nuclei is observed in the form of two pairs of compact details. The nucleus itself, or rather the relativistic electrons surrounding it, is observed as a "point" source.

The difference between the position angles of the fine and hyperfine structure is explained by the gradual rotation of the rotation axes of the nuclei, which are not rigidly connected to the surrounding magnetic fields.[94,121,155]

With increasing distance from the nuclei, the magnetic field intensity falls, so does the energy of the relativistic particles, and the radiation of the components is shifted to lower frequencies.[69] Besides relativistic particles, thermal plasma is ejected from the nuclei, its radiation being observed in the form of emission lines. The nuclei are gravitationally bound and rotate around each other with velocity ~600 km/sec; their period of revolution is $\sim 10^4$ years and their mass is $\sim 10^8 M_\odot$. The large mass and small diameter, ~0.1 pc, indicate that these are supermassive compact bodies of the type of magnetoids[104] or black holes.[211-213]

c) The quasar 3C 273

The quasar 3C 273 is one of the best known quasars. Its red shift is $z = 0.158$, and the distance to it ~500 Mpc. It may be the nucleus of a galaxy.[40] It is one of the first radio sources in whose spectrum a high-frequency excess was observed (see Fig. 1).[7,24,25,114,115] Variability of the radio emission was soon established.[24-28] The characteristic time of variability is several months. It follows that the angular dimensions of the regions of the outbursts are ≤ 0.1 marcsec. The flux density of the radio emission of the individual outbursts reaches tens of janskies. The spectrum of the outburst at the end of 1966 has a bend at millimeter wavelengths.[117] Its angular dimensions must be ~0.05 marcsec.

Besides the compact nucleus, the quasar has an ejection in the direction at angle 223°; it is at a distance 19".5 and measures 10"×2".[130] The spectral index of the ejection is −0.65.[13] The ejection contains dense components, whose spectrum corresponds to component A in Fig. 1; there diameters are ~0".5, and the spectral index of the extended part of the ejection is −2.[38]

Radio interference observations at meter wavelengths with angular resolution 0".1 made it possible to identify

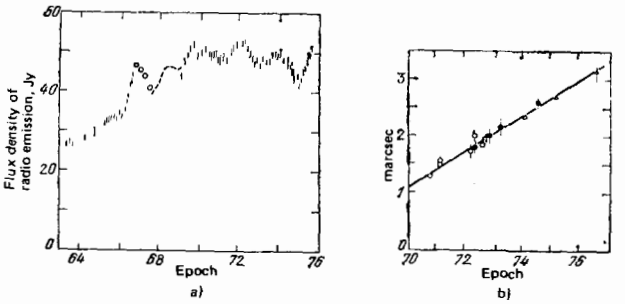

FIG. 14. Change in the flux density of the radio emission of the quasar 3C 273 at wavelength 3.8 cm (a) and change in the distance between the components (b).[95]

a halo of the quasar—component B in Fig. 1.[81,88] At wavelength 75 cm, two components measuring 0".1 × 0".04 and 0".027 × 0".01 with brightness temperatures 10^{10} and 10^{11} °K, respectively, were found.[91,118] A finer structure was observed at 18 cm wavelength[72,78,122,123,136] and 13 cm wavelength.[74,77,92] The two components are separated by 11.3 marcsec in the direction 43°, i.e., in the direction of the ejection. Their diameters are ~2 marcsec and the brightness temperature is $T_b \approx 5 \times 10^{11}$ °K.

Investigations of the quasar using intercontinental baselines with resolution ~1 marcsec at 6 cm made it possible to identify two components separated by 7 marcsec. Betwen them is the nucleus, ~0.4 marcsec, whose spectrum corresponds to component D. The brightness temperature of the nucleus is $T_b \approx 2 \times 10^{12}$ °K.[55,72,78,135] The most complete measurements have been made at 3-cm wavelength. The obtained data showed that at the end of 1970 and the beginning of 1971 the quasar had two components separated by 1.55 marcsec. Their brightness temperature was $T_b \approx 10^{12}$ °K. The fine structure is surrounded by an extended region of ~2.5 marcsec with $T_b \approx 10^{11}$ °K.

The first observations already established motion of the two components relative to one another with velocity $v = (2-10)c$.[127-138] Further observations in 1972–1978 confirmed high separation velocities of $\sim 5.2c$.[93,95] In Table IV, we give the parameters of the two-component model of the quasar 3C 273 in 1975.4–1977.1, and in Fig. 14 we show the change in the distance between the details; the separation velocity is $5.2c$. The separation began at 1967.6 and coincided in time with the increase in the flux density of the radio radiations.[95] It is assumed in Ref. 95 that the additional outbursts of radio emission are partly blended with the radiation of the two components, without, however, significantly changing the basic picture.

TABLE IV.

Epoch	F_0, Jy	$\frac{F_1+F_2}{F_0}$	marcsec	χ, deg	F_1, Jy	marcsec	Ratio of axes	χ_1, deg	F_2, Jy	marcsec	Ratio of axes	χ_2, deg
1975.40	9.07	0.79	1.49	104.6	3.57	0.6	0.8	106	3.55	0.8	0.8	106
1976.14	8.65	0.91	1.59	102.8	4.04	1.1	0.4	114	3.80	0.4	1.0	105
1976.38	8.89	0.80	1.71	103.5	3.92	1.2	1.0	13	3.22	1.3	0.6	161
1976.56	8.84	0.84	1.82	105.9	4.51	1.0	0.8	140	2.91	1.4	0.4	157
1976.73	8.43	1.04	1.69	100.7	5.01	1.2	0.9	139	3.76	0.7	0.6	72
1977.13	8.16	1.04	1.89	100.9	6.37	0.8	0.9	106	2.12	0.8	0.8	106

TABLE V.

Epoch	F_1	F_2	F_3	$\sum_i F_i$	F_0
	Jy				
February 1971	5.4	17.9	19.6	43	51
March 1972	8.9	6.2	21.3	36	
April 1972	7.8	4.8	23.0	36	56
June 1972	6.6	9.5	21.0	37	54
August 1972	8.9	4.7	21.9	36	53
October 1972	9.4	4.8	20.0	34	51
November 1972	6.9	2.0	18.3	38	51

A more complicated but more physical picture is a distribution of radio brightness in which the components are associated with individual outbursts—ejections of high-energy particles.[63,87,94,119,129,131,132] Analysis of the results of observations using the Goldstone-Haystack baseline at wavelength 3.8 cm revealed a three-component distribution of brightness oriented in the direction ~65° with components separated by 0.9 and 1.3 marcsec from the center. Their brightness changes with time, but the relative position remains the same. In Table V, we give the flux densities of the components in 1971–1972.[129] Observations using the Goldstone-Haystack-Alaska radio interferometer in 1972–1973 confirmed the three-component model.[63] A similar conclusion was reached by the authors who investigated the quasar at wavelength 2.8 cm with a multielement interferometer including five radio telescopes during the period 1972–1973. The relative position of the outside components changed by 0.9 marcsec in a year, which corresponds to velocity $v=12c$.[87] In June–July 1974 there was still a three-component structure, and the velocity of the components was the same; Table VI gives the parameters of the model. However, after March 1973 the separation velocity decreased strongly.[132]

Detailed radio charts at the wavelengths 2.8 and 3.8 cm were obtained in 1972–1973 (Fig. 15).[131] During this period, the relative position of the components remained unchanged and was the same at both wavelengths, only the brightnesses changing. In July 1977, the observations were continued at the wavelengths 2.8 and 6 cm.[94] Besides the nucleus, a chain of three components, oriented in the direction of the ejection, is observed.[119] The brightness distribution is approximately the same at the two wavelengths. The spectral index varies from −0.9 in the northeastern part to −0.7 in the southwestern part, while the nucleus has $\alpha=0-1$. At wavelength 50 cm, the ejection reaches ~100 marcsec, and the presence of an antiejection is also confirmed. In 1977.5–1980.6, the structure of the quasar at wavelength at 2.8 and 6 cm was oriented at angle −116° (Fig. 16).[186] The separation velocity of the components during this period was $v=(9.6\pm0.5)c$.

TABLE VI.

	F_0, Jy	F_i, Jy	marcsec	Ratio of axes	χ_i, deg	marcsec	χ, deg
3C 273	44.2	8.1	0.7	1.0	—	0	—
		11.7	0.8	0.6	18	0.94	68
		11.2	2.4	0.5	42	3.21	67
		9.8	3.9	1.0	—	0.3	75

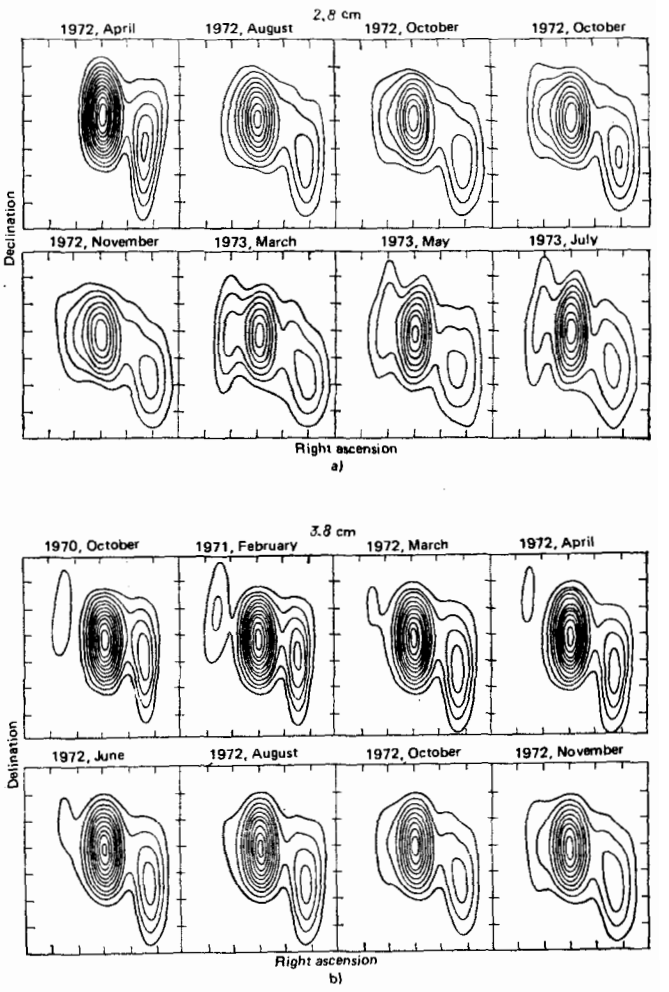

FIG. 15. Detailed charts of 3C 273 at the wavelengths 2.8 cm (a) and 3.8 cm (b).

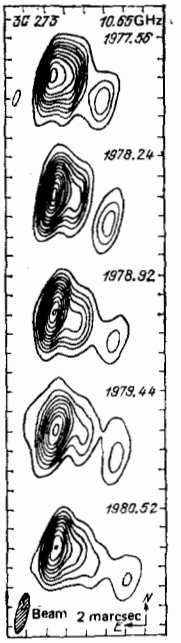

FIG. 16. Distribution of the brightness of 3C 273 at the wavelength 2.8 cm during June 1977–June 1980.[186]

From the velocity of the components, one can estimate the time at which the ejection appeared, which is found to be 1970.1 ± 0.6. At this time, enhanced radio emission was observed. The irregular nature of the variability and the fragmentary data on the structure of the quasar make it impossible to establish a rigorous dependence between them.

At the longer wavelength 50 cm a more extended part of the ejection, ~100 marcsec was found, and the presence of the antiejection observed at shorter wavelengths was confirmed.[94,131,139] In Ref. 185, at wavelength 6 cm, an extended component with position angle different from the small-scale structure was observed.[185]

At short centimeter wavelengths, the structure basically corresponds to the 3-cm data. In Februrary 1973 at wavelength 2 cm three collinearly arranged components had orientation ~63°; their diameters did not exceed 0.7 marcsec and they were separated by 1.4 and 1.6 marcsec from the central component.[119] In 1976–1977 at wavelength 1.35 cm two compact components measuring ~0.2 marcsec and separated by 0.84 marcsec were observed, together with two more extended components whose diameters reached 2.4 and 3.2 marcsec. Their positions correspond to the positions of the details at 3 cm in 1974.5.[133]

Thus, there are two points of view with regard to the dynamics of the quasar 3C 273. According to one of them, there is a change in the brightness of the components, which, however, hardly change their position. According to the second point of view, the outer components are moving apart with an apparent velocity greater than the velocity of light.

d) The quasar 3C 345

The quasar 3C 345 is a fairly strong source of radio emission in the centimeter–millimeter wavelength range. Its red shift is $z = 0.585$, and the distance to it ~2500 Mpc. The spectrum of the quasar is complicated, consisting of three details (Fig. 17). In the case of synchrotron radiation, their angular dimensions must be $\varphi_A = 0''.14$, $\varphi_B = 0''.006$, and $\varphi_C = 0''.001$, respectively. The line part of the spectrum is determined by the extended component. The quasar is surrounded by a halo of ~14 kpc and at a distance of 21 kpc has an ejection in the direction $-31°$. The ejection measures 17 kpc, and its spectral index is $\alpha = -1$.[140,149,151,152] In the same direction as the ejection but at a distance of 13 Mpc a weak source is detected at wavelength 6 cm, the flux density of the radio emission being ~59 mJy; in the opposite direction there is a source with flux ~40 mJy at 11 Mpc. The western source is joined to the nucleus by a "bridge," and between the eastern source and the nucleus there is an intermediate source.

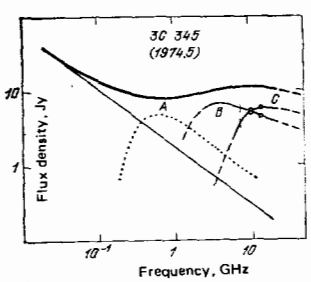

FIG. 17. Spectrum of the quasar 3C 345.[145]

The quasar 3C 345 has a fine structure of its nucleus which consists of several components.[55–57,72,74,77,78,122,127] Their angular dimensions are close to the calculated values $\varphi_A = 2''$, $\varphi_B = 0''.010 \pm 0''.005$, and $\varphi_C \leq 1$ marcsec. According to the data of observations at wavelength 3.5 cm with limiting angular resolution using the Crimea-Goldstone baseline, the diameter of the nucleus is ≤ 0.4 marcsec.[57,72,78] The structure of the source has been represented in the form of a compact nucleus and two components symmetrically placed with respect to it; the brightness temperature of the nucleus is $T_b = 1.5 \times 10^{12}$ °K, and the components are oriented at angle $-103°$.

In Februrary 1974 two components were found to be responsible for the main radiation of the quasar at the wavelengths 2 and 2.8 cm. They were separated by 1.23 marcsec in the direction ~105° and had angular dimensions 0.55 marcsec.[140] During the time that had elapsed since 1971, the distance between the components had changed by 0.37 marcsec.[127] Further observations at 2.8 cm showed that at 1974.15 the separation of the components continued with velocity ~8c.[86,144] A similar phenomenon was observed at 3.8 cm. Comparison of 16 cycles of observations made during 1971–1974 confirmed the superluminal separation of the components at $v = 0.09 \pm 0.03$ marcsec/year or $v = (2.5 \pm 0.8)c$.[64,141,143,145] The direction of the motion hardly changed.

During 1975–1977, observations were made with the Owens Valley–Fort Davis–Green Bank–Algonquin–Effelsberg radio interferometer network at the wavelengths 2.8 and 6 cm.[93,95] Figure 18 shows the correlated fluxes for the Owens Valley–Green Bank radio interferometer. The distance between the minima has increased since 1974.15, and they were not so clearly expressed. This indicates an increase in the angular dimensions of the components, a change in their relative emission, and an increase in the distance between them. Table VII gives models of the source.[93] The change in the distance between the components is shown in Fig. 19. The velocity of the components is $v = (6.7 \pm 0.4)c$. The separation of the components does not depend on the wavelength. The time of ejection of the components corresponds to 1966.3 and the start of the increase in the flux.[117]

An important experiment on the determination of the motion of the source was made using the Haystack–Green Bank–Owens Valley interferometer at wavelength 3.8 cm.[146,147] The position of the quasar 3C 345 was measured relative to the quasar NRAO 512. The position of 3C 345 at the epoch 1950.0 was found to be $\alpha = 16^h41^m17^s.634759$, $\delta = 39°54'10''.95838$, and the relative position of the two sources to be $\Delta\alpha = 2^m29^s.43668 \pm 0.00003$ and $\Delta\delta = 1'40''.726 \pm 0.0003$.

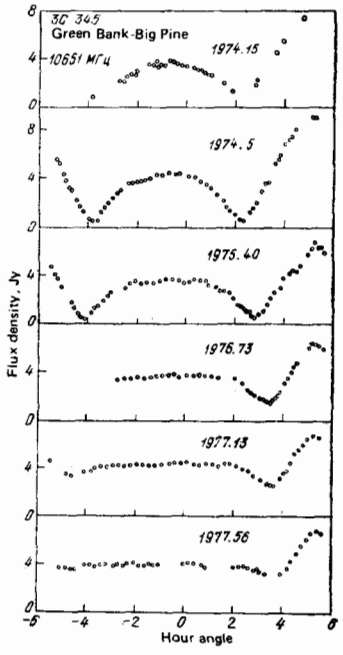

FIG. 18. Correlated fluxes of the source 3C 345. Obtained with the Green Bank–Big Pine radio interferometer during 1974–1977.[95]

The velocity of 3C 345 at the epoch 1973.0 was found to be $v = 0''.00025 \pm 0''.00020$ per year. The accuracy of the obtained results does not yet establish whether there is superluminal velocity of the components of 3C 345, but further observations will resolve this equation.

The emission of the quasar 3C 345 is variable, the variability being irregular.[27,38,132] However, some authors assume that after the outburst in 1967 the flux remained constant. In reality, the enhanced radiation is determined by a large number of outbursts superimposed on one another (see Fig. 19).[134] Thus, the presently observed activity of the nucleus is accompanied by frequenct outbursts of radio emission, and each outburst must correspond to a separate component. In 1977–1979, hybrid charts of the quasar were obtained at the wavelengths 2.8 and 6 cm (Fig. 20).[94,187] The optical thickness of the nucleus is $\tau > 1$, while for the ejection $\tau < 1$. For this reason, the emission of the nucleus is predominantly at shorter wavelengths. Analysis of the observational data at 3.8-cm wavelength confirmed this structure (Fig. 21a). Clouds of particles, observed in the form of a chain of components, are ejected from the nucleus.[154] The determination of the velocity of the components causes certain difficulties in this case, since it is directly related to the

TABLE VII.

Epoch	Distance of components, marcsec	Angle, deg	First component			Second component		
			F, Jy	φ, marcsec	χ, deg	F, Jy	marcsec	χ, deg
1975.40	1.49	104.6	3.57	0.6	106	3.55	0.8	106
1976.14	1.59	102.8	4.04	1.1	114	3.80	0.4	105
1976.38	1.71	105.5	3.92	1.2	13	3.22	1.3	161
1976.56	1.82	105.9	4.51	1.6	140	2.91	1.4	157
1976.73	1.69	100.7	5.01	1.2	139	3.76	0.7	72
1977.13	1.89	100.9	6.37	0.8	106	2.12	0.8	106

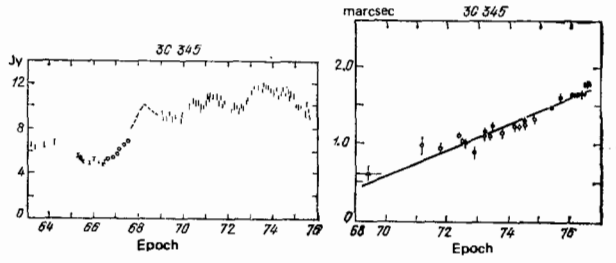

FIG. 19. Change in the flux and the distance between the components in the source 3C 345 at the 3-cm wavelength range.[95]

identification of the details, but $v < c$ has not been found.

At wavelength 1.35 cm, the distribution of the brightness can also be represented in the form of a nucleus and a chain of components ejected from it (Fig. 21b).[133,155] The observations were made with a global network with angular resolution ~0.1 marcsec. The main emission of the quasar at this wavelength is due to its nucleus (~4.7 Jy), whose angular dimensions are ~0.5 marcsec; the greater part of its radiation is associated with an unresolved component measuring ≤ 0.1 marcsec ($F = 3.3$ Jy). The fine structure of the nucleus is shown in the top left-hand corner of Fig. 21b. It consists of the nucleus itself and two compact components displaced relative to it in two opposite directions. The brightness temperature of the nucleus is $\gtrsim 10^{12}$ °K. It is very characteristic that during the considered period component B changed its brightness but kept its position, which agreed with the position at longer wavelengths.

In Ref. 187, a change in the position angle of the ejection from −85° at the nucleus to −75° at distance 3 marcsec from it is noted. At the longer wavelength 6 cm, the position angle was found to be −65°. At the shorter wavelength 1.35 cm, the position angle directly next to the nucleus was −135°. Investigations by means of the global radio interferometer network at 18 cm made it possible to obtain the detailed structure of the ejection and, thus, follow the process of its formation[188,210] (Fig. 21c). Clouds of relativistic particles are ejected along the rotation axis of the nucleus of the quasar in the direction −135°. As they move away, the direction of motion changes from −135° to −65° at a distance of about 5 marcsec. Here there is an accumulation of the particles. Their energy is lower than at the initial time, and they radiate mainly in the decimeter wavelength range. In a preceding period of activity an ejection oriented at angle −31° was formed; it is separated from the nucleus by ~3″.[146,148,149,210] The difference between the position angles is determined by the change of the position angle of the rotation axis of the nucleus of the quasar.

e) BL Lac (VRO 42 22 01)

BL Lac is the nucleus of a giant elliptic galaxy; its red shift is $z = 0.07$.[159] The distance to it is ~300 Mpc. The nucleus is distinguished by an exceptionally high activity, and the change in the flux density of the radio

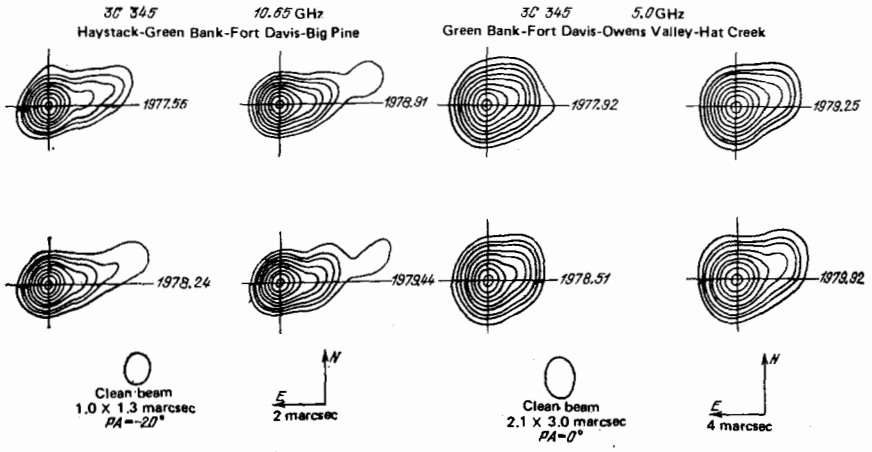

FIG. 20. Hybrid charts of 3C 345 at the wavelengths 2.8 and 6 cm.[93]

radiation in the centimeter wavelength range takes place during a period of a few weeks or even days.[32,34,158,159] The radiation is polarized, and the plane of polarization changes with the same characteristic time. The optical emission is also variable, variations taking place over a time of the order of a day, though even more rapid variations by $0^m.03$ take place over a period of a few minutes.[160,161] Figure 22 shows the change in the flux density at the wavelengths 2.8 and 4.5 cm.[34,157] At the longer wavelengths, the outbursts are delayed by 4–8 days.

The spectrum of the source has a clear excess of radiation down to the shortest millimeter wavelengths. This agrees with the high activity of the nucleus and requires the presence of components of very small angular dimensions. The first observations confirmed this. During September–October 1969, the angular diameter of the source at 6 cm was found to be 0.5 marcsec.[55,78] The observations were made using the intercontinental Crimea–Green Bank baseline.

In February 1971 two components were found in the source at wavelength 3.75 cm; they were separated by 0.9 marcsec in the direction 174°, and the flux density of the radio emission of the components was 8.8 Jy. Observations in June 1971 using the Crimea–Green Bank–Goldstone radio interferometer at wavelength 3.55 cm established that the components had approached each other to 0.5 marcsec. The corresponding velocity was $v=10c$.[56,57] The position angle remained virtually the same. On the basis of the usual models, it was difficult to understand this phenomenon. During the considered period, there was an outburst of radio emission in the source, the start of it corresponding to the middle of May (Fig. 22a). Thus, in June the appearance of a new compact component—a "point" central source—was observed. Its flux must have been 6.8 Jy. Analysis of a three-component model showed that the distance between the outer components was 0.85 marcsec, and the flux of each of them 3.4 Jy. The brightness temperatures of the components were $T_b \approx 1.3\times10^{12}$ for the outer and $T_b \approx 4\times10^{12}$

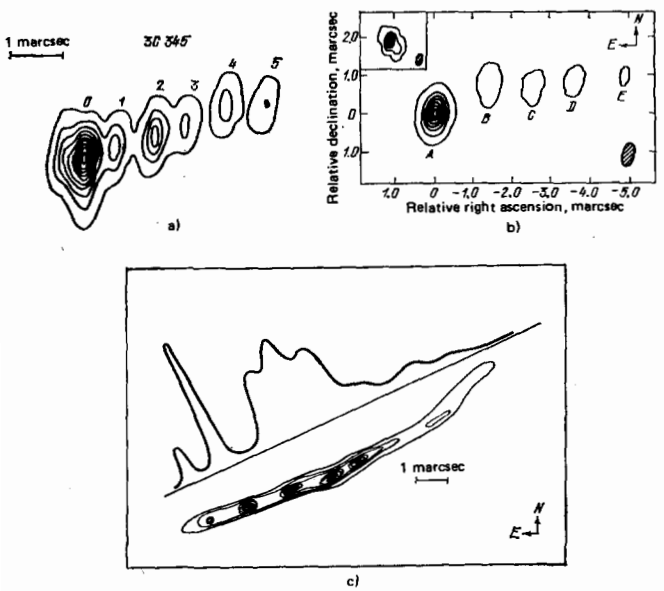

FIG. 21. Distribution of brightness in 3C 345 at the wavelengths 3.7 cm (April 1978,[154]) (a), 1.35 cm (August, 1977) (b),[155] and 18 cm (1980) (c).[210]

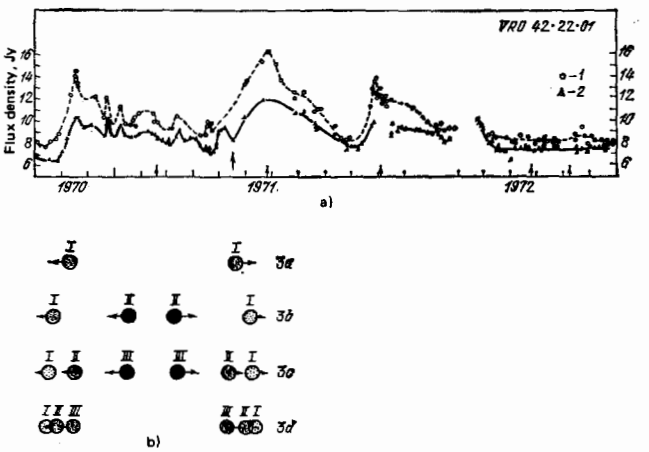

FIG. 22. Change in the flux of the source BL Lac at the wavelengths 2.8 cm (1) and 4.5 cm (2) (a) and model explaining the appearance of the new components (b).[158]

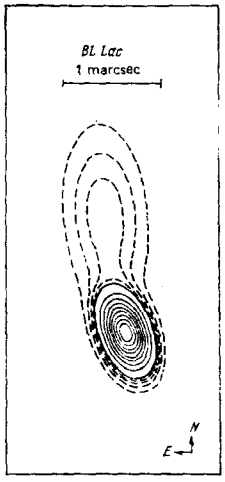

FIG. 23. Synthesized image of the source BL Lac.[132]

for the central component.[56,57,156,38] Further observations in the 3-cm range (the times of observations are indicated by the arrows in Fig. 22) confirmed a complicated structure consisting of pairs of chains of sources moving in opposite directions (see Fig. 28). A pair of components corresponded to each outburst. With increasing distance from the nucleus, the radiation of the components decreases, the components lose velocity, and they pile up.[156,157]

A different model in the form of a nucleus and an ejection is also possible (Fig. 23).[132] Such a distribution was obtained in June–July 1974 at wavelengths 2 and 2.8 cm. At this time, the flux density of the radio emission was near a minimum.[117] The ratio of the fluxes of the components was near 3:1, and the separation of the components in the direction ~10° reached 1.25 marcsec or 2.5 pc. The angular dimensions of the nucleus were 0.2×0.6 marcsec (0.4×1 pc). At 6 cm, the distribution of the brightness was similar.[132]

f) The radio source OJ 287

The radio source OJ 287 is a BL Lacertae object. In its nucleus there are active rapidly varying processes accompanied by outbursts of optical and radio emission.[162-164] A phase of high activity began in 1970.5 and lasted to the end of 1975. Changes in the radio emission takes place over a few days and even a few hours, which requires exceptionally small angular dimensions of the outbursts.[117] The rapid variability of the radio emission of the source makes it difficult to construct its spectrum, simultaneous observations being required. However, one can distinguish in the spectrum two components—a high-frequency and a low-frequency component (Fig. 24).[38] The low-frequency part hardly changes and has a maximum at ~1 GHz; the high-frequency part is subject to appreciable changes. It passes through a maximum at around ~20 GHz, the flux density of the radio radiation at this point being in the interval (4–10) Jy. In this case, the angular dimensions of this region must be ~0.1 marcsec. The red shift of the object is not known, and therefore the distance to it cannot be determined. However, knowing the dimensions of the components, the angular distances between them, and the durations of the outbursts, one can make corresponding estimates, which give a distance of ~200 Mpc.[38] Observations using the transcontinental Goldstone-Haystack interferometer at wavelength 3.8 cm in February 1971 showed that the source is effectively unresolved, <1 marcsec.[127] It was also unresolved with the intercontinental Crimea-Goldstone baseline.[56,57] Its diameter was ≤0.15 marcsec, and $T_b \geq 4\times10^{12}$ °K. Directly before the observations an outburst was observed in the source; this lasted for ~0.1 year, which agrees with the obtained result. Later observations at 3 cm confirmed the compactness of the source; in May 1974, its diameter was 0.3 marcsec, and its flux 6 Jy.[86] In February 1974, the corresponding values were 0.6 marcsec and $F=4$ Jy, and in July 1974 they were 0.4 marcsec and $F=3.2$ Jy.[132] One observed a decrease in the angular dimensions of the source with increasing flux density of the radio emission, which indicates the presence of a more extended component, its diameter being several milliseconds of arc; the spectral index is −1 (Ref. 89) and corresponds to the low-frequency component.

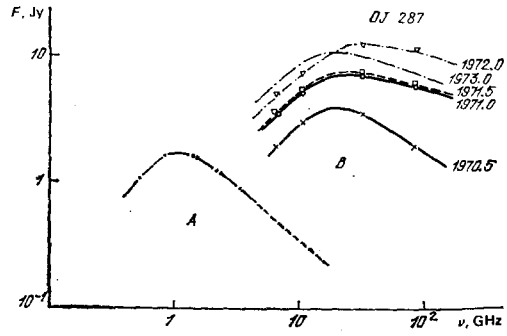

FIG. 24. Spectrum of the source OJ 287.[38]

g) The quasar 3C 279

The quasar 3C 279 has red shift $z=0.538$, and its emission is variable.[117] Its structure has been studied in detail by VLBI.[74,77,78,90,92,124,127,138,165] The structure of the quasar consists of four components corresponding to the details in its spectrum. Component *A* determines the long-wavelength part of the radiation, B the decimeter part, C the short-wavelength part, and, finally, D the part with highest frequency. The angular dimensions of the components are $\varphi_B = 22$, $\varphi_C = 1$, and $\varphi_D = 0.4$ marcsec. The two last components are associated with the fine structure of the nucleus. During 1969–1972 the distance between the compact components was found to change with velocity $v=(8-20)c$, and after 1972 even with $45c$.[189] However, further detailed observations, including some at 2 cm, established that the double source is only an approximate model. In reality, there are three collinearly arranged components separated from each other by 2.2 marcsec. The position of the components is stationary, but their relative brightness changes.[119,129]

h) The quasar 4C 39.25

The quasar 4C 39.25 has $z = 0.698$, and is at a distance of ~3000 Mpc. Its spectrum has a high-frequency excess and varies with time. At centimeter wavelengths one observes emission of two compact components separated by (2.02 ± 0.05) marcsec. The angular diameters of the sources are ~0.3 marcsec, their brightness temperature is $T_b \approx 10^{12}$ °K, and the position angle is 81°. The fine structure is surrounded by an extended region of ~20 marcsec, and its radiation is predominant at decimeter wavelengths. The structure of the source remained unchanged during 1972–1975.[56,57,78,140,145,167]

i) The quasar 3C 454.3

The quasar 3C 454.3 has $z = 0.859$. The high-frequency part of the spectrum is determined by the emission of a compact nucleus measuring ~0.2 marcsec and a halo measuring ~0.4 marcsec. At decimeter wavelengths, its dimensions increase to 200 marcsec (wavelength 75 cm). Depending on the stage of the activity of the nucleus, the fine structure can be represented in the form of an elongated ellipse with axes 1× 9.5 marcsec or two components separated by 3.5 marcsec in the direction 115°.[55,77,78,86,89,122,127,132,140] The last investigations in the centimeter wavelength range show that the structure hardly changes with time, the brightness of the details merely changing.[86]

j) NRAO 150

NRAO 150 is an unidentified object, has a complicated spectrum, and consists of three details. At decimeter wavelengths, the emission of component B, whose diameter is 10–15 marcsec, is predominant. At centimeter wavelengths a three-component collinear structure is observed. Two components are separated by 1.1 marcsec and their brightness temperature is $T_b \approx 10^{12}$ °K; the diameter of the third is 0.7 marcsec and $T_b \approx 10^{11}$ °K. The position angle of the source is ~60° (Fig. 25).[56,57,78,89,132,133,140] The nucleus is oriented at angle ~152°, the ratio of its axes is 0.6, and the length of the major axis is 0.2 marcsec. The length of the major axis of the second component is 0.4 marcsec, and the ratio of the axes is 0.7. The position angles of the components differ from the position angle of the structure as a whole. The distribution of the brightness remained unchanged during 1972–1975.[167]

k) Simple structure of nucleus

A simple structure of the nucleus is observed in the giant elliptic galaxy M 87 (the radio source Virgo A) and the nearest galaxy to it, which is M 81. The angular dimensions of the nucleus of M 87 decrease with the wavelength from 1″ at meter wavelengths to ~6 marcsec at decimeter wavelengths and ~0.3 marcsec at centimeter wavelengths. The diameter of the nucleus at centimeter wavelengths is 3×10^3 a.u., and its brightness temperature is $T_b \approx 10^{11}$ °K.[38,56,57,74,77,104] The change in the angular dimensions with the wavelength

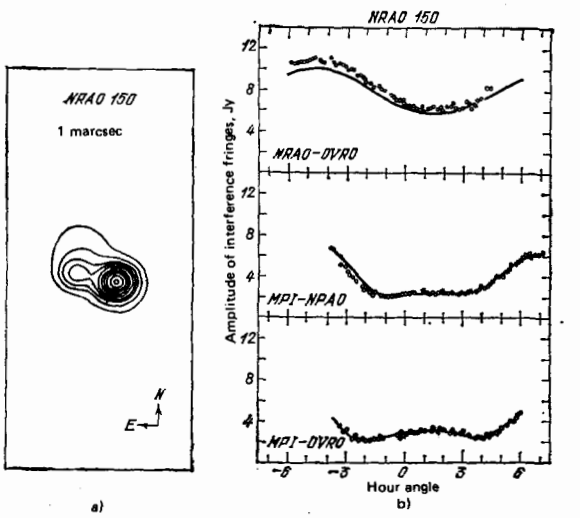

FIG. 25. Distribution of the radio brightness in the source NRAO 150 (a) and the corresponding correlated fluxes obtained with radio interferometers (b).[140]

as $\sim\lambda^2$ is determined by the electron energy distribution and the magnetic field intensity. Such a dependence can also occur in the case of scattering of the radiation of a compact source by inhomogeneities of an ionized medium, but in this case the brightness temperature of the unscattered source will reach exceptionally high values at meter wavelengths, considerably in excess of the Compton limit.[38] The diameter of the nucleus of M 81 is ~1300 a.u., and $T_b \approx 2 \times 10^{10}$ °K; if we take a brightness temperature equal to the Compton limit, then its diameter is ~200 a.u.[168]

The low brightness temperature of the nuclei of objects of this type is probably due to their insufficiently high activity. This does not rule out their having had a much higher activity earlier, as is indicated by the ejection of a jet of matter from the nucleus of M 87.[214] The length of the jet reaches ~22″.

There is also a clear ejection of matter from the elliptic galaxy NGC 6251, which has $z = 0.023$.[166] Observations of the object were made with the new instrument in New Mexico, and its fine structure was investigated by a radio interferometer network in the United States. The brightness distribution of the object is shown on different scales in Fig. 26. The position angle of the ejection is (300.5 ± 2)°. The emission of the large-scale components is predominant in the decimeter range; the emission of the small scale details, in the centimeter range. The brightness temperature of the fine structure is $T_b \approx 5 \times 10^{11}$ °K.

5. DISCUSSION OF RESULTS

The fine structure of objects with active nuclei is directly determined by the activity of their nuclei. In the case of low activity, one observes the emission of the relativistic plasma surrounding these nuclei; the diameters of these regions are ~0.01 pc, the magnetic field intensity is $H = 10^{-5\pm2}$ Oe, the energy of the relativistic particles is $E = 10^{54\pm3}$ erg, and $T_b \approx 10^{11}$ °K. The

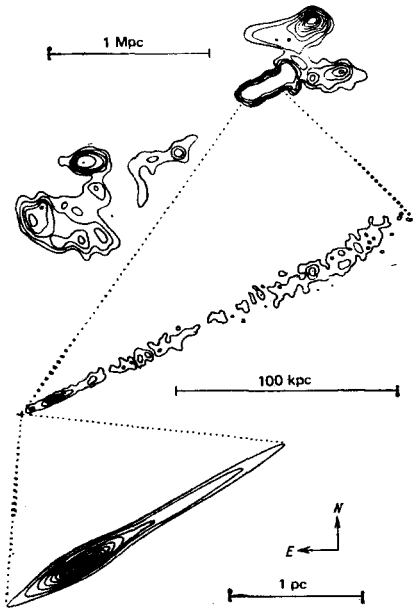

FIG. 26. Structure of the source NGC 6251.[166]

nuclei of the galaxies M 81 and M 87 are objects of this type.

Bright compact components are associated with more active processes in the nuclei and correspond to ejections of clouds of relativistic particles, which give outbursts of radio emission. To each cloud of relativistic particles there corresponds a bright compact source. In the case of sufficiently frequenct repetition of the ejections, they can be observed in the form of a string of components, which become a jet, as, for example, in the quasar 3C 345.[210] The active nucleus is itself also observed in the form of a compact component. Components can be observed symmetrically placed with respect to the nucleus, but, as a rule, one-sided ejections are observed; in many cases, this also applied to the large-scale structure-the ejections in 3C 273, 3C 345, Virgo A, and others. The dimensions of the individual components are several tens of parsecs, and their brightness temperatures are $T_b \approx 10^{12}$ °K, even reaching $\sim 10^{13}$ °K in the initial stages. Especially bright components are observed at decimeter wavelengths,[30,67] but their nature is not clear.

As a rule, apparent superluminal velocities of the components are associated with two-component structures. This is the case for the sources 3C 120, 3C 273, 3C 345, and others. It follows from the latest studies that the simplified models are not sufficiently accurate, and models in the form of one-sided ejections or two components with different fluxes reflect the observational data better. In particular, this applies to 3C 345, but even in this case the velocity of the components may exceed the velocity of light. The apparent velocity of the components in the objects 3C 120, 3C 273, and 3C 279 is in the interval $5c \leq v \leq 40c$.

The magnetic field intensities associated with the outbursts is $H = 0.01-0.1$ Oe, and the energy of the relativistic particles $E \approx 10^{52}$ erg.[145] The maximal radiation of the outbursts is in the centimeter-millimeter wavelength range. In some cases, the duration of the outbursts does not exceed a few months, and sometimes even a few days. According to the polarization observations, the ejection of matter takes place along the magnetic field for the objects 3C 120, 3C 273, 3C 345. In other objects such a dependence is not observed, but this may be due to a different orientation of the magnetic field near the nucleus.[47,132]

The observed superluminal separation velocities of the components have been considered in many papers (see Refs. 44, 47, 79, 113, 150, 170–173, 175, 176, 185, and 204) and can be given the following explanations:

1. Rapid motion of the components.

2. A significant deviation of the Hubble constant or a noncosmological origin of the red shirt of the objects, and also inaccuracy of the cosmological model.[190-192]

3. An echo effect: reflection of radiation.[116]

4. A gravitational lens.[193,194]

5. A systematic change in the optical thickness of the object.[195]

6. Synchrotron or curvature radiation of electrons in a dipole magnetic field.[196-198]

7. Various kinematic illusions associated with the finite signal propagation time.[8,199]

The last explanation is the one that has been most widely accepted.[8,200] Initially, this model was used to interpret the rapid variability of the radio emission. The radio source was represented in the form of an expanding cloud of relativistic particles. Because of the finite propagation time of the radiation, the duration of an event in a source moving with near luminal velocity will be $\gamma = (1-\beta^2)^{-0.5}$ times shorter for an external observer.[44,47,113] The observed angular diameter will be $\sim\gamma$ times smaller, and its brightness temperature T_b will be $\sim\gamma^2$ times greater. This last result is due to the fact that the emission of the source becomes anisotropic and takes place in a cone of width $\varphi \sim \gamma^{-1}$. Accordingly, the observed flux density of the radio emission is increased compared with a source at rest by

$$\frac{F_b(\theta)}{F_0} = \gamma^3 (1-\beta\cos\theta)^{\alpha-3} \text{ times.}$$

The values of the observed fluxes for different β are shown as functions of the angle θ in Fig. 27.[201]

In the case $\sin\theta = 1/\gamma$ and $\alpha = 0$ the flux density of the radio emission of a source moving toward the observer is $F_b \approx 8\gamma^3 F_0$, while for one moving away it is $F_b \approx \gamma^{-3} F_0/8$. This phenomenon is considered in detail in Ref. 44 Simultaneously with the change of the apparent emission there is a change in the velocity. The apparent velocity of a cloud of relativistic particles moving with velocity v will be[185,202]

$$v_\perp = \frac{v\sin\theta}{1-\beta\cos\theta}.$$

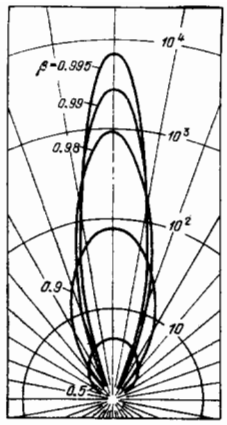

FIG. 27. Directionality of the emission of a source moving with near luminal velocity.[201]

Figure 28 shows the dependence of $v_\perp$ on β and θ. For $\theta = 90°$, the influence of the finite signal propagation time on the apparent velocity is slight and $v_\perp \approx v$. But for $\theta \approx 1/\gamma$ the apparent velocity is equal to the maximal value $v_\perp \approx \gamma v$. The observed velocities can significantly exceed the velocity of light. Thus, this model explains both the high brightness temperatures and the velocities. However, the velocities $v \sim c$ also give rise to a number of problems.[203]

1. One needs additional energy in the form of the kinetic energy of the cloud of relativistic particles and the magnetic field energy.

2. The cloud of relativistic particles is within a region that emits optical emission lines, and if the cloud moves with such velocity it will interact with the surrounding medium, which must lead to a significant change of the spectral lines.

3. The high velocity leads to a high directionality of the emission and a correspondingly small probability of observation of the phenomenon. But many objects are observed with variability of the radio emission, limiting brightness temperatures, and superluminal motions.

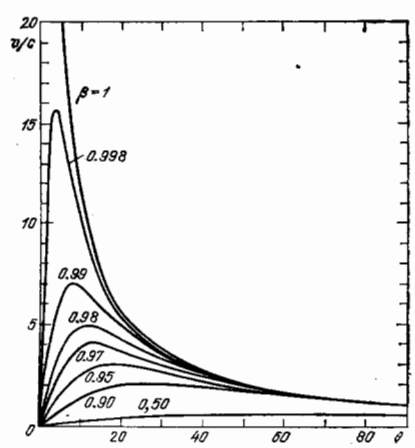

FIG. 28. Apparent velocity v/c of the source as a function of the direction θ and the velocity of its motion (β).[201]

4. The observed flux densities of the radio emission of the components are nearly equal in magnitude (two-component model), whereas they should differ appreciably at the measured values of the velocities.

All these difficulties can be largely attributed to the insufficiently complete picture of the observed phenomena. At the present time we have at our disposal only the first data about the fine structure of the nuclei of active objects and their evolutionary development. And by no means always do they make it possible to follow the evolution of the outbursts in a wide range of radio wavelengths. It is very probable that the components moving away from us are indeed not seen because of the effect of the directed emission. This could explain the asymmetry of the ejections, but only in the initial stage. After the loss of velocity, both components should be seen. This point of view was put forward for the first time to explain the asymmetry of the ejections in the objects M 87 and 3C 273.[205,206] The observed second component could be the nucleus itself. It should also be noted that the number of sources in which motion of components with high velocity has been measured is small. Indirect estimates of possible superluminal motion based on high brightness temperatures of the components are not convincing and could have a different explanation; in particular, incoherent synchrotron radiation permits such high temperatures.[182] In this connection, great importance attaches to measurement of the velocities of the components and their variation in time, as follows from the majority of models. However, it has not yet been possible to establish deceleration.[113,150] In the presence of fairly frequenct outbursts observed at different distances from the nucleus, it is difficult to eliminate the possibility of apparent superluminal motion of the components.[208] Such a phenomenon is observed in the galaxy 3C 84.[65,69,120,130] The position of the components is determined by the structure of the magnetic field.[69,180]

Extended components, whose dimensions reach several parsecs, are found at large distances from the nucleus and are the result of accumulation of particles generated during many outbursts; they are the result of generation during definite epoch of activity. Usually the brightness temperature of these components does not exceed $T_b \approx 10^{11}$ °K, and their magnetic field is $H \approx 10^{-3}$ Oe. The maximal emission is at decimeter and partly centimeter wavelengths. The energy of the particles is $E \approx 10^{61}$ erg.[145]

The emission of both the compact and the extended components is determined by the synchrotron mechanism. Differences between the properties of the components of different objects are not obersved. Supercompact components correspond to the initial stage of the ejection of particles, and their high brightness temperature, which exceeds the limiting 10^{12} °K, can be explained by a near luminal velocity. On the other hand, the high brightness temperature may exceed the limiting value and be determined by the energy of the electrons and the stability of the magnetic field.[182]

One of the most important questions in the investiga-

tion of objects with active nuclei is the question of the source of the high-energy particles, the source of the energy of the nucleus and the mechanism of its transformation into relativistic particles, and the mechanism of ejection of particles to distances of hundreds of kiloparsec. The source of energy could be a compact star cluster, an accreting black hole,[211-213] or a supermassive rotating magnetoplasma body—a magnetoid. This supermassive rotator, whose rotational, thermal, and magnetic energies are approximately equal, is a generator of high-energy particles.[47,179] The generation of the particles is determined by the interaction of the relativistic and thermal plasma with the magnetic field. A strong low-frequency electromagnetic wave accelerates particles to energies $E/Mc^2 \approx 10^3$.[179] The irregular ejection of matter is due to stretching of the magnetic lines of force. In this way the gravitational energy of the massive body is transformed into relativistic particles. Such a model corresponds to the observational data—the unchanged position angle of the direction of the ejections within a definite epoch of activity of a nucleus.[38,69] Thus, the position angle of the hyperfine structure characterizes the position of the rotation axis of the magnetoid or some other supermassive body, for example, a black hole. A change in the position of the rotation axis of the nucleus could be due to the ejection of huge amounts of matter during each of the periods of activity. The mass losses reach $M/M \approx 10^{-7}$ per year, and the mass of a nucleus is 10^7–$10^9 M_\odot$.[177]

Exceptional possibilities for investigating the nuclei of quasars, BL Lacertae objects, and galaxies have been opened up by VLBI. They have been found to have a complicated structure and to vary with time. It is possible that they are objects of only one class, differing only in the scales of the activity of their nuclei or the phase of the activity. At the present time, systematic observations are being made of these objects using radio interferometer networks in a wide range of radio wavelengths. This will make it possible to study both the small- and the large-scale structures and to understand the process of their formation and evolution. When space radio telescopes are out into orbit around the Earth and space communication lines are established, it will be possible to obtain images of individual outbursts with the necessary angular resolution. The first steps in this direction have already been taken.[54,174,181,183]

[1]K. I. Kellermann and I. I. K. Pauliny-Toth, Proc. IEEE **61**, 1174 (1973).
[2]K. I. Kellermann and I. I. K. Pauliny-Toth, Astrophys. J. **155**, L71 (1969).
[3]G. Greenstein, H. H. Chu, and J. V. Narlikar, Superstars [Russian translation], Mir, Moscow (1965).
[4]V. A. Razin, Izv. Vyssh. Uchebn. Zaved. Radiofiz. **4**, 584 (1960).
[5]V. A. Razin, Izv. Vyssh. Uchebn. Zaved. Radiofiz. **6**, 921 (1960).
[6]V. I. Slish, Nature **199**, 682 (1963).
[7]G. L. Verschuur and K. I. Kellermann (eds.), Galactic and Extragalactic Radio Astronomy, Springer, New York (1974).
[8]M. J. Rees, Nature **211**, 468 (1966).
[9]K. I. Kellermann, Ann. Phys. (N.Y.) **336**, 1 (1980).
[10]K. I. Kellermann, in: The Physics of Non-Thermal Radio Sources (Ed. G. Setti), D. Reidel, Dordrecht, Holland (1976).
[11]G. Hazard, M. V. Mackey, and A. J. Shimmins, Nature **197**, 1037 (1963).
[12]G. G. Getmantsev and V. L. Ginzburg, Zh. Eksp. Teor. Fiz. **4**, 20 (1950).
[13]G. B. Sholomitskiĭ, N. F. Sleptsova, and L. I. Matveenko, Astron. Zh. **42**, 1135 (1965) [Sov. Astron. **9**, 882 (1965)].
[14]J. I. Schmidt, Nature **218**, 663 (1968).
[15]M. Cohen, Ann. Rev. Astron. Astrophys. **7**, 619 (1969).
[16]K. R. Lang, Astrophys. J. **164**, 249 (1971).
[17]L. T. Little and A. Hewish, Mon. Not. R. Astron. Soc. **134**, 221 (1966).
[18]L. T. Little and A. Hewish, Mon. Not. R. Astron. Soc. **136**, 393 (1968).
[19]W. M. Cronyn, Thesis D. Ph., Univ. of Maryland (1970).
[20]M. H. Cohen and E. J. Gundermann, Astrophys. J. **155**, 645 (1969).
[21]M. H. Cohen, E. J. Gundermann, and D. E. Harris, Astrophys. J. **150**, 767 (1967).
[22]V. L. Ginzburg, Dokl. Akad. Nauk SSSR **162**, 42 (1965) [Sov. Phys. Dokl. **10**, 420 (1965)].
[23]V. V. Virkevich and V. I. Shishov, Tr. Fiz. Inst. Akad. Nauk SSSR **62**, 42 (1972).
[24]V. I Kostenko and L. I. Matveenko, Astron. Zh., **6**, 1181 (1968) [*sic*].
[25]V. I. Kostenko and L. I. Matveenko, Izv. Vyssh. Uchebn. Zaved. Radiofiz. **10**, 1467 (1970).
[26]W. A. Dent and T. T. Haddock, Nature **205**, 4970 (1965).
[27]W. A. Dent, Science **148**, 1458 (1965).
[28]K. I. Kellermann and I. I. K. Pauliny-Toth, Ann. Rev. Astron. Astrophys. **6**, 417 (1968).
[29]W. J. Medd, B. H. Andrew, G. A. Harvey, and J. L. Locke, Mon. Not. R. Astron. Soc. **77**, 109 (1972).
[30]R. Fanti *et al.*, Astron. Astrophys. Suppl. Ser. **36**, 359 (1979).
[31]W. L. Williams *et al.*, Astrophys. J. **173**, L147 (1972).
[32]E. E. Epstein *et al.*, Astrophys. J. **178**, L51 (1972).
[33]G. A. Seielstad, Astrophys. J. **193**, 55 (1975).
[34]J. M. Macloed, B. H. Andrew, W. J. Medd, and E. T. Olen, Astrophys. J. **9**, 19 (1971).
[35]G. A. Harvey, B. H Andrew, J. M. Macloed, and W. J. Medd, Astrophys. Lett. **11**, 147 (1972).
[36]I. I. Pronik, Astron. Zh. **51**, 1204 (1974) [Sov. Astron. **18**, 717 (1975)].
[37]I. I. Pronik, Astron. Zh. **54**, 260 (1977) [Sov. Astron. **21**, 144 (1977)],
[38]L. I. Matveenko, Avtoreferat dokt. dissertatsii (Author's Abstract of Doctoral Dissertation), D-021052, Moscow (1978).
[39]R. W. Hobbs, J. P. Holinger, and G. E. Marandino, Astrophys. J. **154**, L49 (1968).
[40]S. Wyckoft *et al.*, Astrophys. J. **242**, L59 (1980).
[41]H. van der Laan, Nature **211**, 1131 (1966).
[42]D. S. De Yong, Astrophys. J. **177**, 573 (1972).
[43]F. W. Peterson and W. A. Dent, Astrophys. J. **186**, 421 (1973).
[44]L. M. Ozernoĭ and V. A. Sazonov, Astrophys. Space Sci. **3**, 365 (1969).
[45]I. S. Shklovskiĭ, Astron. Zh. **54**, 713 (1977) [Sov. Astron. **21**, 401 (1977)].
[46]I. S. Shklovskiĭ, Astron. Zh. **42**, 30 (1965) [Sov. Astron. **9**, 22 (1965)].
[47]L. M. Ozernoĭ and L. É. Ulanovskiĭ, Astron. Zh. **51**, 8 (1974) [Sov. Astron. **18**, 4 (1974)].
[48]R. A. Syunyaev, Astron. Zh. **48**, 244 (1971) [Sov. Astron. **15**, 190 (1971)].
[49]R. A. Syunyaev and Ya. B. Zel'dovich, Astrophys. Space Sci. **7**, 20 (1971).

[50]L. I. Matveenko, N. S. Kardashev, and G. B. Sholomitskiĭ, Izv. Vyssh. Uchebn. Zaved. Radiofiz. **8**, 651 (1965).
[51]R. Batchelor *et al.*, Pis'ma Astron. Zh. **2**, 467 (1976) [Sov. Astron. Lett. **2**, 181 (1976)].
[52]L. I. Matveenko *et al.*, Pis'ma Astron. Zh. **4**, 51 (1978) [Sov. Astron. Lett. **4**, 26 (1978)].
[53]V. I. Kostenko and L. I. Matveenko, Preprint No. 340 [in Russian], Institute of Space Research, USSR Academy of Sciences, Moscow (1977).
[54]N. S. Kardashev, S. V. Pogrebenko, and G. S. Tsarevskiĭ, Preprint No. 449 [in Russian], Institute of Space Research, USSR Academy of Sciences, Moscow (1978).
[55]D. D. Broderik *et al.*, Astron. Zh., **47**, 784 (1970) [Sov. Astron. **14**, 627 (1971)].
[56]D. D. Brokerik *et al.*, Preprint No. 117 [in Russian], USSR Academy of Sciences, Moscow (1972).
[57]L. I. Matveenko *et al.*, Astron. Zh. **50**, 1157 (1973) [Sov. Astron. **17**, 731 (1974)].
[58]B. G. Clark, Ann. Rev. Astron. Astrophys. **8**, 115 (1970).
[59]D. N. Fort and H. K. Yee, Astron. Astrophys. **50**, 19 (1976).
[60]W. D. Cotton, Astron. J. **84**, 1122 (1979).
[61]A. C. S. Readhead and P. Wilkinson, Astron. J. **223**, 25 (1978).
[62]J. A. Högbom, Astron. Astrophys. Suppl. **15**, 417 (1974).
[63]A. E. E. Rogers *et al.*, Astrophys. J., **193**, 293 (1974).
[64]J. J. Wittels *et al.*, Astron. J. **81**, 933 (1976).
[65]I. I. K. Pauliny-Toth *et al.*, Nature **259**, 17 (1976).
[66]R. C. Jennison, Mon. Not. R. Astron. Soc. **118**, 276 (1958).
[67]R. Genzel *et al.*, Astrophys. J. **247**, 1039 (1981).
[68]I. I. Shapiro *et al.*, Astron. J. **84**, 1459 (1979).
[69]L. I. Matveenko *et al.*, Pis'ma Astron. Zh. **6**, 77 (1980) [Sov. Astron. Lett. **6**, 42 (1980)].
[70]L. I. Matveenko, Preprint No. 479 [in Russian], Institute of Space Research, USSR Academy of Sciences, Moscow (1979).
[71]N. C. Mathur, M. D Grossi, and M. R. Pearlman, Radio Sci. **5**, 1253 (1970).
[72]K. I. Kellermann *et al.*, Astrophys. J. **153**, L209 (1968).
[73]K. I. Kellermann and I. K. Pauliny-Toth, Astron. J. **73**, 874 (1968).
[74]K. I. Kellermann *et al.*, Astrophys. J. **161**, 803 (1970).
[75]D. L. Jauncey *et al.*, Astrophys. J. **160**, 337 (1970).
[76]D. B. Shaffer, M. H. Cohen, D. L. Jauncey, and K. I. Kellermann, Astrophys. J. **173**, L147 (1972).
[77]J. J. Broderick, K. I. Kellerman, B. B. Shaffer, and D. L. Jauncey, Astrophys. J. **172**, 299 (1972).
[78]K. I. Kellermann, Astrophys. J. **169**, 1 (1971).
[79]T. Kogure, Publ. Astron. Soc. Jpn. **23**, 449 (1971).
[80]W. A. Dent, Astrophys. J. (Lett.) **175**, L55 (1972).
[81]W. C. Erickson *et al.*, Astrophys. J. **177**, 101 (1972).
[82]A. C. S. Readhead and A. Hewish, Mon. Not. R. Astron. Soc. **78**, 1 (1974).
[83]K. I. Kellermann *et al.*, Astrophys. J. **183**, L51 (1973).
[84]S. M. Bhandary, S. Ananthakrishnan, R. A. Prames, Aust. J. Phys. **27**, 121 (1974).
[85]V. K. Kapahi, M. N. Joshi, and N. V. Sarma, Astron. J. **79**, 515 (1974).
[86]J. J. Wittels *et al.*, Astrophys. J. **196**, 13 (1975).
[87]R. T. Schilizzi *et al.*, Astrophys. J. **201**, 263 (1975).
[88]T. A. Clark *et al.*, Astron. J. **80**, 923 (1975).
[89]D. B. Shaffer and R. T. Schilizzi, Astron. J. **80**, 753 (1975).
[90]M. H. Cohen *et al.*, Nature **268**, 405 (1977).
[91]J. A. Galt *et al.*, Mon. Not. R. Astron. Soc. **178**, 301 (1977).
[92]J. Gabbary *et al.*, Astrophys. J. **215**, 20 (1977).
[93]G. A. Seielstad, Astrophys. J. **229**, 53 (1979).
[94]A. C. S. Readhead *et al.*, Astrophys. J. **231**, 299 (1979).
[95]M. H. Cohen *et al.*, Astrophys. J. **231**, 293 (1979).
[96]M. H. Cohen *et al.*, Astrophys. J. **201**, 249 (1975).
[97]V. S. Troitskiĭ, Usp. Fiz. Nauk **109**, 771 (1973) [Sov. Phys. Usp. **16**, 286 (1974)].
[98]L. I. Matveenko, Itogi nauki i tekhniki. Ser. Astronomiya (Reviews of Science and Technology. Astronomy Series), VINITI, Moscow (1977).
[99]I. I. Shapiro *et al.*, Astrophys. J. **183**, L47 (1973).
[100]L. Bell, Nature **270**, 386 (1977).
[101]M. J. Rees, Astrophys. J. **2**, 1 (1968).
[102]M. J. Rees, Nature **211**, 468 (1966).
[103]T. H. Legg *et al.*, Nature **244**, 18 (1973).
[104]W. C. Erickson *et al.*, Astrophys. J. **177**, 101 (1972).
[105]G. K. Miley and G. C. Perola, Astron. Astrophys. **45**, 223 (1975).
[106]D. N. Fort, Astrophys. J. **207**, L155 (1976).
[107]I. I. K. Pauliny-Toth *et al.*, Nature **259**, 17 (1976).
[108]R. Minkowsky, Radio Astronomy: IAU Symp. **4**, 107 (1957).
[109]E. M. Burbidge and G. R. Burbidge, Astrophys. J. **142**, 1351 (1965).
[110]V. C. Rubin, W. K. Fort, Ch. K. Peterson (Jr.), and J. H. Oort, Astrophys. J. **211**, 693 (1977).
[111]É. A. Dibaĭ, Astrofizika **46**, 725 (1968).
[112]J. Romney, Thesis D. Ph., Caltech (1979).
[113]K. I. Kellermann, Ann. Phys. (N.Y.) **336**, 1 (1980).
[114]A. Kh. Barret, B. G. Kutuza, L. I. Matveenko, and A. E. Salomonovich, Astron. Zh. **42**, 527 (1965) [Sov. Astron. **9**, 418 (1965)].
[115]V. I. Kostenko and L. I. Matveenko, Astron. Zh. **43**, 280 (1966) [Sov. Astron. **10**, 225 (1966)].
[116]D. Lynden-Bell, Nature **270**, 396 (1977).
[117]B. H. Andrew, J. M. MacLeod, G. A. Harvey, and W. W. Medd, Astron. J. **83**, 863 (1978).
[118]R. W. Clarke *et al.*, Mon. Not. R. Astron. Soc. **146**, 381 (1969).
[119]A. E. Niel, K. I. Kellermann, B. G. Clark, and D. B. Shaffer, Astrophys. J. (Lett.) **197**, L109 (1975).
[120]E. Preuss *et al.*, Astron. Astrophy. **79**, 268 (1979).
[121]M. H. Cohen and A. C. S. Readhead, Astrophys. J. **233**, L101 (1979).
[122]B. G. Clark *et al.*, Astrophys. J. **153**, L67 (1968).
[123]J. M. Morgan *et al.*, Astrophys. J. **153**, 151 (1968).
[124]C. A. Knight *et al.*, Science **172**, 52 (1971).
[125]V. A. Efanov, A. G. Kislyakov, I. G. Moiseev, and A. V. Naumov, Astron. Zh. **15**, 2 (1971) [*sic*].
[126]T. H. Legg *et al.*, J. R. Soc. Can. **65**, 176 (1971).
[127]M. H. Cohen *et al.*, Astrophys. J. **170**, 207 (1971).
[128]A. J. Legg *et al.*, Nature 235, 147 (1972).
[129]K. I. Kellermann *et al.*, Astrophys. J. (Lett.) **189**, L19 (1974).
[130]R. G. Conway and D. Stannard, Nature **255**, 310 (1975).
[131]T. H. Legg *et al.*, Astrophys. J. **211**, 21 (1977).
[132]K. I. Kellermann *et al.*, Astrophys. J. **211**, 658 (1977).
[133]I. I. K. Pauliny-Toth *et al.*, Pis'ma Astron. Zh. **4**, 64 (1978) [Sov. Astron. Lett. **4**, 32 (1978)].
[134]J. J. Wittels *et al.*, Astron. J. **83**, 560 (1978).
[135]K. I. Kellermann *et al.*, Astrophys. J. **189**, L19 (1978).
[136]B. G. Clark, M. H. Cohen, and D. L. Jauncey, Astrophys. J. **149**, L151 (1967).
[137]M. H. Cohen, Astrophys. J. **12**, 81 (1972).
[138]A. R. Whitney *et al.*, Science **171**, 227 (1971).
[139]P. N. Wilkinson, A. C. S. Readhead, B. Anderson, and G. H. Purcell, Astrophys. J. **232**, 360 (1979).
[140]D. B. Shaffer *et al.*, Astrophys. J. **201**, 256 (1979).
[141]J. J. Wittels *et al.*, Astrophys. J. **206**, L75 (1976).
[142]E. J. Wampler, L. B. Robinson, E. M. Burbidge, and J. A. Baldwin, Astrophys. J. **198**, L52 (1975).
[143]M. H. Cohen and S. C. Unwin, in: Extragalactic Radio Sources (Eds. D. S. Heeshen and C. M. Wade), Symp. IAU (1981), p. 255.
[144]M. H. Cohen *et al.*, Astrophys. J. **206**, L1 (1976).
[145]D. B. Shaffer *et al.*, Astrophys. J. **218**, 218 (1977).
[146]C. R. Menuyk *et al.*, Astron. J. **220**, L27 (1978).

[147]I. I. Shapiro *et al.*, Astron. J. **84**, 1459 (1979).
[148]T. J. Pearson, A. C. S. Readhead, and P. Wilkinson, Astrophys. J. **236**, 714 (1980).
[149]R. A. Perley and K. J. Johnston, Astron. J. **84**, 1247 (1979).
[150]T. D. Kinman, Nature **267**, 798 (1977).
[151]R. J. Davis, D. Stannard, and R. G. Conway, Mon. Not. R. Astron. Soc. **185**, 435 (1978).
[152]R. J. Davis, D. Stannard, and R. G. Conway, Nature **267**, 696 (1977).
[153]L. I. Matveenko *et al.*, Pis'ma Astron. Zh. **6**, 662 (1980) [Sov. Astron. Lett. **6**, 347 (1980)].
[154]J. J. Wittels *et al.*, in: Symposium of IAU–VLBI, Heidelberg (1978).
[155]L. B. Baath *et al.*, Astrophys. J. (Lett.) **243**, L123 (1981).
[156]B. G. Clark *et al.*, Astrophys. J. **182**, L55 (1973).
[157]B. H. Andrew, Astrophys. J. **186**, L3 (1973).
[158]B. H. Andrew *et al.*, Astrophys. J. **191**, 51 (1974).
[159]J. B. Oke and J. E. Gunn, Astrophys. J. (Lett.) **189**, L5 (1974).
[160]D. Dupuy *et al.*, Astrophys. J. **156**, L135 (1969).
[161]R. Racine, Astrophys. J. **159**, L99 (1970).
[162]P. D. Usher, Astron. J. **84**, 1253 (1979).
[163]B. H. Andrew, G. A. Harvey, and W. J. Medd, Astrophys. J. (Lett.) **9**, 151 (1971).
[164]T. D. Kinman *et al.*, Astron. J. **79**, 349 (1974).
[165]W. D. Cotton *et al.*, Astrophys. J. **229**, L115 (1979).
[166]A. C. S. Readhead, M. H. Cohen, and R. D. Blanford, Nature **272**, 131 (1978).
[167]L. R. Baath *et al.*, Astron. Astrophys. **86**, 364 (1980).
[168]K. I. Kellermann *et al.*, Astrophys. J. **210**, L21 (1976).
[169]A. C. S. Readhead, P. N. Wilkinson, and G. H. Purcell, Astrophys. J. **215**, L13 (1977).
[170]W. A. Christiansen and J. S. Scott, Astrophys. J. **216**, L1 (1977).
[171]R. D. Blanford, C. F. McKee, and M. J. Rees, Nature **267**, 211 (1977).
[172]S. M. Chitre and J. V. Narlikar, Mon. Not. R. Astron. Soc. **187**, 655 (1979).
[173]D. S. De Young, Astrophys. J. (Lett.) **8**, 43 (1971).
[174]R. Preston, in: Symposium at Heidelberg, September (1978).
[175]V. N. Kurilchik, Astrophys. J. (Lett.) **10**, 115 (1972).
[176]F. W. Peterson and W. A. Dent, Astrophys. J. **186**, 421 (1973).
[177]G. Burbidge and J. Perry, Astrophys. J. **205**, L55 (1976).
[178]L. I. Matveyenko *et al.*, Preprint No. 644 [in English]; Institute of Space Research, Moscow (1981); Sov. Lett. Astron. J. **8**, 470 (1981).
[179]L. M. Ozernoĭ, Usp. Fiz. Nauk **120**, 309 (1976) [Sov. Phys. Usp. **19**, 863 (1976)].
[180]B. V. Komberg and V. M. Lyutyĭ, Pis'ma Astron. Zh. **6**, 7 (1980) [Sov. Astron. Lett. **6**, 3 (1980)].
[181]T. Clark, in: Symposium at Heidelberg, September (1978).
[182]É. I. Tsvetanov and V. M. Charugin, Astron. Zh. **58**, 3 (1981) [Sov. Astron. **25**, 1 (1981)].
[183]J. L. Yen *et al.*, Science **198**, 289 (1977).
[184]R. C. Walker *et al.*, Astrophys. J. **243**, 589 (1981).
[185]T. J. Pearson *et al.*, Quoted in Ref. 143, p. 355.
[186]T. S. Pearson *et al.*, Nature **290**, 365 (1981).
[187]M. H. Cohen *et al.*, Astrophys. J. **247**, 774 (1981).
[188]L. I. Matveenko *et al.*, Pis'ma Astron. Zh. **8**, 148 (1982) [Sov. Astron. Lett. **8**, 77 (1982)].
[189]I. I. K. Pauliny-Toth *et al.*, Preprint MPI (1981).
[190]I. E. Segal, Astrophys. J. **227**, 15 (1979).
[191]G. R. Burbidge, Phys. Scr. **17**, 281 (1978).
[192]K. I. Kellermann and D. B. Shaffer, in: Colloquium IAU No. 37; Q. Bulkowsky and Q. Westerbend (Eds.), L' Evolution des Galaxies et ses Implications Cosmologiques, CNRS, Paris, p. 347.
[193]J. M. Barnothy and M. F. Barnothy, BAAS **3**, 472 (1979).
[194]S. M. Chitre and J. V. Narlikar, Astrophys. J. **235**, 335 (1980).
[195]R. I. Epstein and M. J. Geller, Nature **265**, 219 (1977).
[196]M. Milgrom and J. N. Bahcall, Nature **274**, 349 (1978).
[197]R. H. Sanders and L. N. DaCosta, Astron. Astrophys. **70**, 477 (1978).
[198]J. N. Bahcall and M. Milgrom, Astrophys. J. **236**, 24 (1980).
[199]A. Cavaliere, P. Morrison, and Sortori, Science **173**, 525 (1971).
[200]M. J. Rees, Mon. Not. R. Astron. Soc. **135**, 345 (1967).
[201]M. Ryle and M. S. Longair, Mon. Not. R. Astron. Soc. **136**, 123 (1967).
[202]V. L. Ginzburg, Teoreticheskaya fizika i astrofizika (Theoretical Physics and Astrophysics), Nauka, Moscow (1981), Chap. 9.
[203]T. W. Jones and G. R. Burbidge, Astrophys. J. **186**, 791 (1973).
[204]A. P. Marscher and J. S. Scott, Publ. Astron. Soc. Pacific **92**, 127 (1980).
[205]I. S. Shklovskiĭ, Astron. Zh. **40**, 972 (1963) [Sov. Astron. **7**, 748 (1963)].
[206]I. S. Shklovskiĭ, Astron. Zh. **42**, 30 (1965) [Sov. Astron. **9**, 22 (1965)].
[207]P. A. Scheuer and A. C. S. Readhead, Nature **277**, 182 (1979).
[208]W. A. Dent, Science **175**, 1105 (1972).
[209]L. M. Ozernoĭ and V. I. Shishov, Pis'ma Astron. Zh. **6**, 269 (1980) [Sov. Astron. Lett. **6**, 149 (1980)].
[210]L. I. Matveyenko *et al.*, in: IAU VLBI Symposium (1982).
[211]M. C. Begelman, R. D. Blanford, and M. J. Rees, Nature **287**, 307 (1980).
[212]K. S. Thorne and R. D. Blanford, Quoted in Ref. **143**, p. 255.
[213]D. L. Meiler, Quoted in Ref. 143, p. 263.
[214]M. J. Reid *et al.*, Quoted in Ref. 143, p. 293.

Translated by Julian B. Barbour